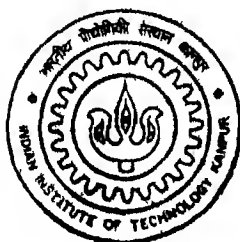


# **Preparation of Thick PZT Films by Sol Gel Method Using PVP as a Processing Aid and Their Characterization**

by  
**SHYAM DHAR DUBEY**



TH  
MS/2001/M  
2857/p

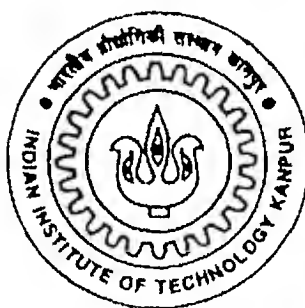
**MATERIALS SCIENCE PROGRAMME**  
**INDIAN INSTITUTE OF TECHNOLOGY, KANPUR**

**January, 2001**

# **Preparation of Thick PZT Films by Sol Gel Method Using PVP as a Processing Aid and Their Characterization**

*by*

**SHYAM DHAR DUBEY**



**MATERIALS SCIENCE PROGRAMME**

**Indian Institute of Technology Kanpur**

**JANUARY, 2001**

7 : 1/MS

भा  
जति - 133647



A133647

---

# **Preparation of Thick PZT Films by Sol Gel Method Using PVP as a Processing Aid and Their Characterization**

*A Thesis Submitted  
in Partial Fulfillment of the Requirements  
for the Degree of*

**MASTER OF TECHNOLOGY**

*in*

**MATERIALS SCIENCE**

*by*

**SHYAM DHAR DUBEY**

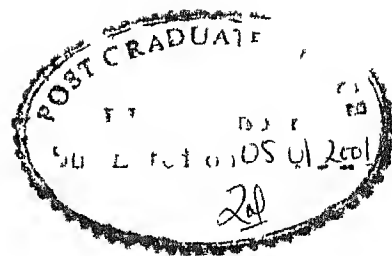
*to the*

**MATERIALS SCIENCE PROGRAMME**

**Indian Institute of Technology Kanpur**

**JANUARY, 2001**

# Certificate



This is to certify that the present work entitled **Preparation of Thick PZT Films by Sol Gel Method using PVP as a Processing Aid and their Characterization** by Mr Shyam Dhar Dubey has been carried out under my supervision and to the best of my knowledge it has not been submitted elsewhere for a degree

  
Dr D C Agrawal

Professor  
Materials Science Programme  
IIT Kanpur 208016

*Dedicated to*

*My Parents*

# Acknowledgements

I take this opportunity to express my sincere regards and gratitude to **Dr D C Agrawal** for his excellent guidance constant inspiration and encouragement throughout project work He has not only supervised my project but also built in me the confidence to plan and work independently He has always without exception spared his precious time for me whenever I needed his help and guidance I am indeed fortunate to get an opportunity of working with him

I am grateful to Thapa ji and Uma Shankar ji for their ready help and cooperation in the laboratory

Joyful company of my classmates juniors and friends Mani Pandey Ramanujam Amit Neeraj Kundu Santosh Sahoo S Dutta A Dalvi Ashutosh Tiwari Abhishek Anil Ajay Arvind Mohan and Sharad will always remind me of the glorious days of my stay at IIT Kanpur

Shyam Dhar Dubey

## **ABSTRACT**

The sol gel process has been used with polyvinyl pyrrolidone (PVP) as an additive to prepare films of lead zirconate titanate (PZT) on Si substrates. The PVP (monomer)/Ti molar ratio is varied from 0 to 2. Two sol concentrations (0.32 and 0.63 M) have been used. Thickness of the film is found to increase with the initial addition of PVP and becomes nearly a constant as the PVP concentration is further increased. The film thickness is very sensitive to the sol concentration, increasing nearly linearly with it. Films of thickness about  $0.5\ \mu\text{m}$  without cracks can be obtained in a single coating using PVP (monomer) / Ti molar ratio between 0.5 to 1.5 and a sol concentration of 0.63. This can be compared with the thickness of  $\sim 0.1\ \mu\text{m}$  which can be deposited by single coating without using PVP. The dielectric constant of the films increases rapidly on increasing the PVP (monomer)/ Ti ratio from 0 to  $\sim 0.5$  and then becomes nearly constant. Higher dielectric constant ( $\sim 150$ ) is obtained in films prepared using the more concentrated sol than that ( $\sim 75$ ) prepared using the thinner sol. The dielectric constant is found to be nearly constant at frequency  $> 30\ \text{KHz}$  but increases steeply as the frequency is decreased. The films have significantly higher dielectric loss than thin films prepared without PVP using low concentration sol. It is found that the concentration of the acetic acid plays an important role in determining the dielectric loss. The dielectric constant of the films is found to increase with the film thickness from about 150 for  $4\ \mu\text{m}$  thick film to  $\sim 350$  for a  $11.5\ \mu\text{m}$  thick film. The electrical conductivity of the films was studied by impedance spectroscopy at different temperatures. At higher temperatures the Cole Cole plots showed two arcs corresponding to grain and grain boundary conduction. The data has been analyzed to obtain the conductivity of the grains and the grain boundaries.



# CONTENTS

## 1 Introduction

1 1	Ferroelectric crystals	1
1 2	PZT ferroelectric ceramics	1
1 3	Effect of electrical field	5
1 4	Hysteresis loop	5
1 5	Applications of ferroelectric PZT materials in device technology	7
1 6	Ferroelectric thick films	9
1 6 1	Effect of thickness on properties of PZT films	
1 6 1 1	Effect of thickness on ferroelectric properties	10
1 6 1 2	Effect of thickness on C V characteristics	14
1 6 1 3	Thickness dependent leakage current density	15
1 6 1 4	I V characteristic of thick films	16
1 6 2	Processing of thick films	
1 6 2 1	Screen-printing	17
1 6 2 2	Thick PZT glass film composite by plasma sprayed method	18
1 6 2 3	PZT thick film by aerosol deposition method (ADM)	18
1 6 2 4	Thick film by electrophoretic deposition	19
1 6 2 5	Thick film by interfacial polymerization	19
1 6 3	PZT thick film by sol gel	
1 6 3 1	The sol gel process	20
1 6 3 1 1	Hydrolysis mechanism	21
	Acid catalyzed hydrolysis	22
	Base catalyzed hydrolysis	22
1 6 3 1 2	Condensation mechanism	23
1 6 3 2	Sol gel process for thick films	24
1 6 3 2 1	By using diol and acetylacetonate	24
1 6 3 2 2	Thick films by using tri alkoxy silanes	25
1 6 3 2 3	Thick films by using progressive (step wise) -heating schedule	25
1 6 3 2 4	Thick films by using suitable substrate	25
1 7	Statement of problem	

## 2 Experimental procedures

2 1	Introduction	27
2 2	Sample preparation	
2 2 1	Silicon wafer cleaning	28
2 2 2	Deposition of $ZrO_2$ film over Si(100) substrate by spin coating	28
2 2 2 1	$ZrO_2$ sol preparation	30
2 2 2 2	Deposition of $ZrO_2$ film	32
2 2 3	Deposition of Au-Pd bottom electrode on $ZrO_2$ /Si (100) by sputtering	32
2 2 4	Deposition of thick films of PZT on Au Pd / $ZrO_2$ /Si(100) substrate by spin coating	33
2 2 4 1	Preparation of PZT sol	35
2 2 4 2	PZT thick film deposition	39
2 3	Characterization	
2 3 1	X Ray diffraction	41
2 3 2	Complex impedance analysis	42
2 3 2 1	Introduction	42
2 3 2 2	Measurements	45
2 3 3	Dielectric constant	46

## 3 Results and discussion

3 1	X-ray diffraction	48
3 2	Effect of PVP/Ti ratio	50
3 3	Impedance spectroscopy	51
	<b>Conclusion</b>	80
	<b>References</b>	82
<b>Appendix</b>	(1) Silicon wafer cleaning	86
	(2) Calculation of the amount of ingredients used for the preparation of sol for $ZrO_2$ coating	87
	(3) Calculation of the amount of ingredients used for the preparation of sol for $Pb_{1.05}(Zr_{0.535}Ti_{0.465})O_3$ (PZT) coating	89

## List of Figures

Fig No	Title	Page No
1 1	Phase diagram for PZT	2
1 2	Pervoskite structure of Pb (ZrTi)O <sub>3</sub>	3
1 3	Effect of cooling below the Curie temperature	4
1 4	Various crystal structures in PZT ceramic	4
1 5	Hysteresis loop (Electrical field vs polarization	5
1 6	Effect of temperature (T ) on nature of Hysteresis loop of ferroelectric thin film	6
1 7	(a) Capacitor without dielectric materials (b) Capacitor with ferroelectric materials	8
1 8	Effect of electric field on ferroelectric domain wall	8
1 9	Effect of thickness on hysteresis loop i.e saturation polarization and remnant polarization	10
1 10	Plot between relative dielectric constant vs temperature for different thickness	11
1 11	Applied electric field vs polarization for different thickness (0.25 0.50 2.0 $\mu$ m)	12
1 12	Applied electrical field vs polarization for different thickness (5 7 10 $\mu$ m)	13
1 13	(a) Polarization (P <sub>r</sub> ) and Coercive field (E <sub>C</sub> ) vs film thickness (b) Film thickness vs saturation polarization	15
1 14	C-V characteristics of PZT hetero layers films	14
1 15	Hydrolysis and condensation reaction	21
1 16	Acid catalyzed hydrolysis mechanism	22
1 17	Base catalyzed hydrolysis mechanism	23
1 18	Role of chelating agent [Only two -OCH <sub>3</sub> group takes part in hydrolysis reaction Other two -OCH <sub>3</sub> group are protected by acetylacetonate (chelating group)]	24
2 1	Flow chart diagram for ZrO <sub>2</sub> sol preparation	31
2 2	Schematic of the Au/Pd/PZT/Au/Pd/ZrO <sub>2</sub> /Si (100) sample	33
2 3	(a) Tensile stress evolution and crack formation in gel under heat treatment (b) Condensation and pore collapse in gel films under heat treatment	34
2 4	Poly(vinylpyrrolidone) PVP and N-vinyl-2-pyrrolidone (VP)	34
2 5	PVP inhibiting the condensation reaction in gel films by protecting the -OH group by carbonyl group PVP	35

2 6	Flow Chart for Sol Preparation of $\text{Pb}_{1.05}(\text{Zr}_{0.535}\text{Ti}_{0.465})\text{O}_3$ with PVP	37
2 7	Au Pd/PZT/Au Pd/ZrO <sub>2</sub> /Si (100) sample preparation	40
3 1	X ray diffractogram of ZrO <sub>2</sub> thin films deposited on Si(100) n type substrate (annealing temperature is 650 °C)	56
3 2	(a) X ray diffractogram of PZT films deposited on Au Pd/ZrO <sub>2</sub> /Si(100) n type substrate ( annealing temperature is 650 °C)	57
	(b) X ray diffractogram of PZT films with PVP (PVP/Ti=1 0) deposited on Au Pd/ZrO <sub>2</sub> /Si(100) n type substrate ( annealing temperature is 650 °C)	58
3 3	Effect of PVP/Ti ratio and sol concentration on film thickness	59
3 4	Frequency vs dielectric loss for PZT with different PVP/Ti monomer molar ratio (sol concentration is 0 63M)	60
3 5	Frequency vs dielectric loss for PZT with different PVP/Ti monomer molar ratio (sol concentration is 0 32M)	61
3 6	Effect of sol concentration and PVP/Ti ratio on dielectric loss	62
3 7	Effect of PVP/CH <sub>3</sub> COOH ratio on dielectric loss	63
3 8	Effect of thickness on dielectric loss of PZT (PVP/Ti=1 0) Sol concentration 0 63M	64
3 9	Frequency vs dielectric constant for PZT with different PVP/Ti ratio	65
3 10	Frequency vs Dielectric loss for PZT with different PVP/Ti ratio (Sol concentration 0 63M)	66
3 11	PVP/ti molar ratio vs dielectric constant	67
3 12	Effect of thickness on dielectric constant (Sol concentration 0 63M)	68
3 13	Cole Cole plot for PZT (no PVP) at different temperatures (Sol concentrartion=0 32M)	69
3 14	Cole Cole plot for PZT (PVP/Ti=0 2) at different temperatures (Sol concentration=0 32M)	70
3 15	Cole Cole plot for PZT(PVP/Ti=0 5M) at different temperatures (Sol concentration=0 32M)	71
3 16	Cole Cole plot for PZT (PVP/Ti=1 0) at different temperatures (sol concentration=0 32M)	72
3 17	Cole Cole plot for PZT (PVP/Ti=1 5) at different temperatures (Sol concentration =0 32M)	73
3 18	Cole Cole plot for PZT(PVP/Ti =2 0) at different temperatures (sol concentration =0 32M)	74
3 19	DC Conductivity associated with grain interior of PZT with PVP present in sol in different PVP/Ti molar ratio (sol concentration=0 32M)	75
3 20	DC Conductivity associated with grain boundary of PZT with PVP present in sol in different PVP/Ti molar ratio (sol concentration=0 32M) (Sol concentration=0 32M)	76

3 21	Cole Cole plot for PZT (PVP/Ti =2 0) [Sol concentration =0 63M]	77
3 22	Cole Cole plot for PZT (PVP/Ti =1 5 [Sol concentration =0 63M]	78
3 23	Cole Cole plot for PZT (PVP/Ti =1 0) [Sol concentration =0 63M]	79

## LIST OF TABLES

Table no	Title	Page no
2 1	Specification of the chemical used for sol preparation for $\text{ZrO}_2$ coating	30
2 2	Chemical used for $\text{Pb}_{1.05}(\text{Zr}_{0.535}\text{Ti}_{0.465})\text{O}_3$ sol preparation	36
2 3	Amount of PVP for PZT with different PVP (monomer)/ $\text{Ti}$ molar ratio	36
3 1	X ray diffraction data for PZT (Perovskite structure)	49
3 2	DC conductivity of bulk and grain boundary for PZT with different PVP/ $\text{Ti}$	54
3 3	Activation energy for PZT with different PVP/ $\text{Ti}$ ratio	55

# **Chapter 1**

## **1 INTRODUCTION**

### **1.1 Ferroelectric crystals**

On the basis of geometry the crystals can be divided into seven crystal systems which are further divided into 32 point groups based on symmetry. Out of these 32 point groups 11 have center of symmetry i.e. these crystals have no polarity and the remaining are non-centro-symmetric. Thus out of these 21, 20 show piezoelectricity (stress/strain dependent polarization) and 10 point groups out of these 20 are pyroelectric and exhibit temperature dependent polarization. Some pyroelectric materials also show ferroelectric properties. The most important property of ferroelectric materials is the presence of a hysteresis loop, the graph between the polarization and applied electrical field. The polarization is reversed upon reversal of the applied electrical field and a certain polarization called the remnant polarization is present upon removal of the external field. All the ferroelectric materials also exhibit piezoelectric properties.

### **1.2 PZT ferroelectric ceramics**

Lead Zirconate Titanate (PZT) has the perovskite structure ( $ABX_3$ ). In the perovskite structure of  $ABX_3$ ,  $A^{+2}$  ( $Pb^{+2}$ ) occupies the corner positions of the cube.  $X^{2-}$  ( $O^{2-}$ ) ions

occupy the face centered positions and  $B^{+4}(Zr^{+4}/Ti^{+4})$  occupy the body centered position (Fig1 2) PZT can be considered as a solid solution of lead zirconate  $PbZrO_3$  and  $PbTiO_3$ . The single crystals of the ceramic are ferroelectric (F) paraelectric (P) or antiferroelectric (A) and have cubic (C) tetragonal (T) or rhombohedral(R) crystal structure depending on the composition and temperature (Fig1 1). Various crystal structures are related as shown in fig (1 4). Optimum ferroelectric and piezoelectric properties are obtained near the morphotropic phase boundary (MPB) corresponding to the composition  $Pb(Zr_{0.535}Ti_{0.465})O_3$  with excellent ferroelectric properties.

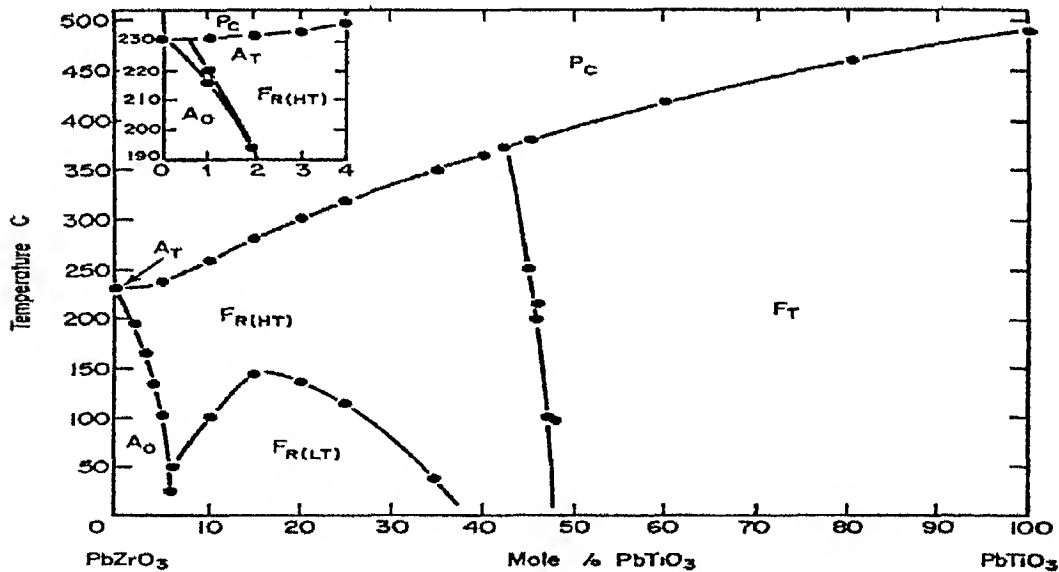


Fig 1 1 Phase diagram for PZT [31]



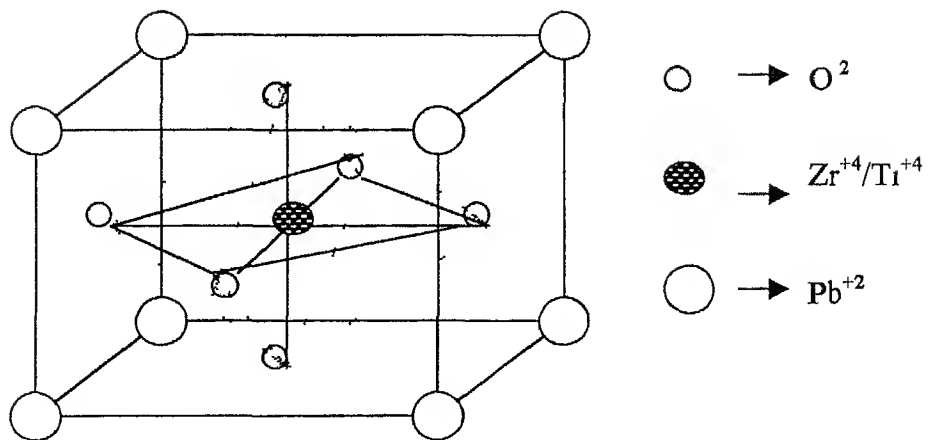


Fig1 2 Pervoskite structure of  $Pb(ZrTi)O_3$

Above a temperature called Curie temperature PZT has cubic structure and in this case the centers of the negative ions and the body centered positive ions coincide. As a result there is no spontaneous dipole moment in the cubic structure. If the crystal is cooled below the Curie temperature the  $B^{+4}$  ion is shifted to one side of the body centered position while the oxygen ions (negatively charged ions) are shifted in opposite direction. Due to this shift local dipole moment is created throughout the crystal (Fig 1 3). The dipoles of neighboring unit cells are aligned producing a large polarization in regions of the crystal called domains. However the domains themselves are randomly aligned so there is no net polarization.

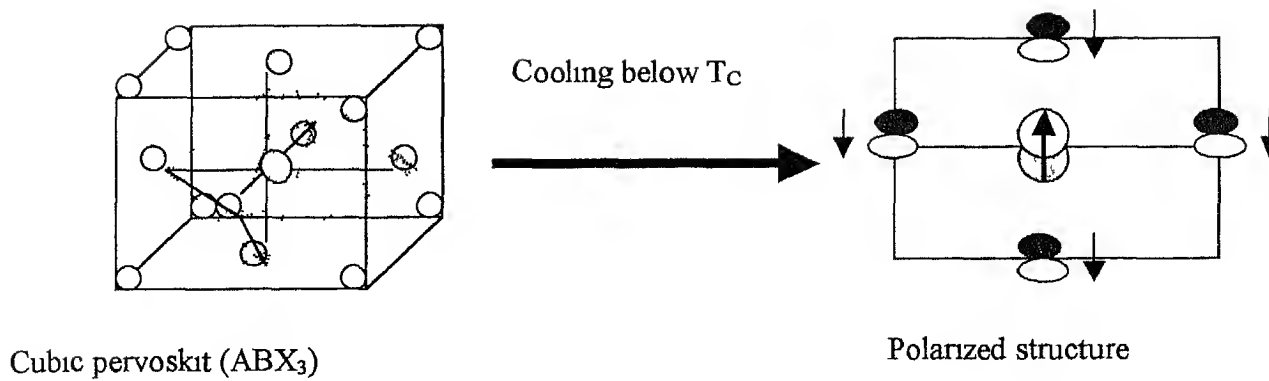


Fig1 3 Effect of cooling below the Curie temperature

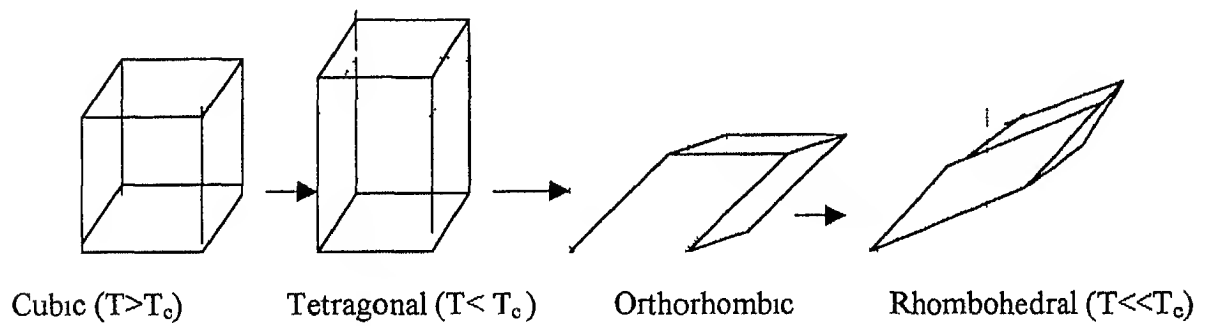


Fig1 4 Various crystal structures in PZT ceramic

To explain the ferroelectric properties of materials curie law was utilized with little modification (Curie Weiss law)

$$\chi = \frac{N\mu^2}{3K(T - T_c)}$$

$T_c$  = Curie temperature

$\chi$  = susceptibility and  $\mu$  = dipole moment

Alignment of dipoles begins spontaneously at critical temperature ( $T_c$ ) called Curie temperature. Aligning of the dipoles in a parallel array with field increases the effective polarization.

### 1.3 Effect of electrical field

At room temperature the  $ABO_3$  crystal exhibits no net polarization in the absence of external electrical field i.e. the ferroelectric domains are oriented randomly in the crystal which results in no net dipole moment. When an electrical field is applied the domains tend to align in the direction of the electrical field. Thus a net dipole moment is created in the direction of the electrical field. Thus a net dipole moment is created. This is called poling.

### 1.4 Hysteresis loop

Hysteresis loop represents the relation between the polarization and the electrical field.

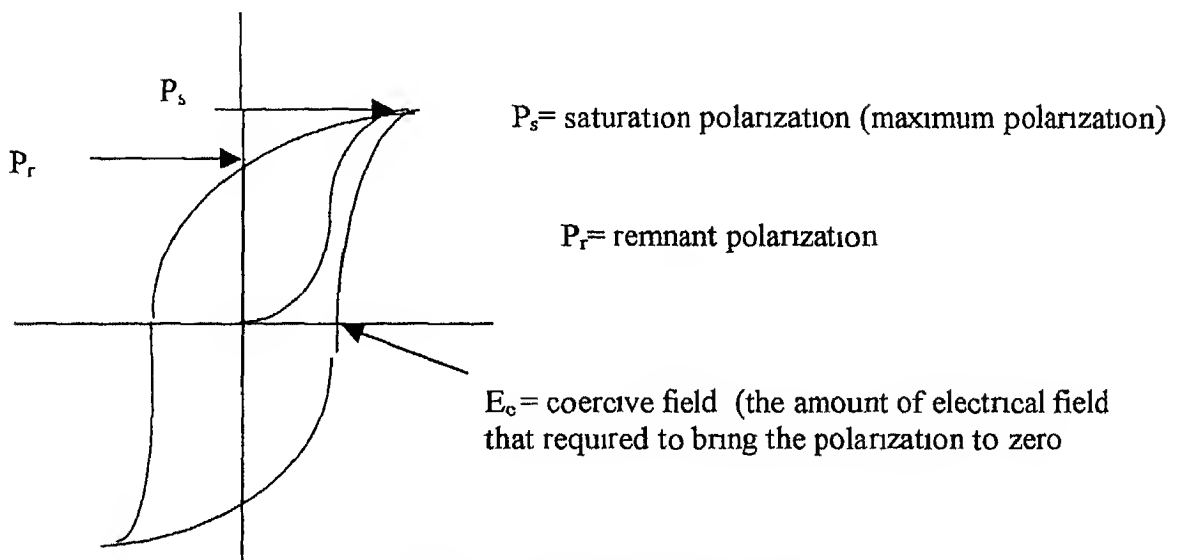


Fig 1.5 Hysteresis loop (electrical field vs polarization)

It is the most important characteristic of ferroelectric materials. In figure (1.7 and 1.8) there is no polarization at zero electric field in the virgin material. On applying an external electrical field, the polarization spontaneously increases with increase in the electrical field. After some value of the electrical field, the polarization reaches a nearly constant value called the saturation polarization ( $P_s$ ). On decreasing the electrical field to zero, there is still some polarization remaining in the sample; this is called remnant polarization ( $P_r$ ). Increasing the field in the negative direction brings the polarization to zero position. This value of the field is called the coercive field ( $E_c$ ). On further increasing the negative electrical field, the polarization reaches a negative saturation value ( $P_s$ ). Coming back to zero electrical field, a negative remnant polarization results. Thus electrical field vs polarization plot is a hysteresis loop.

The nature of the hysteresis loop for ferroelectrical materials is also strongly dependent on temperature relative to the Curie temperature (Fig. 1.6).

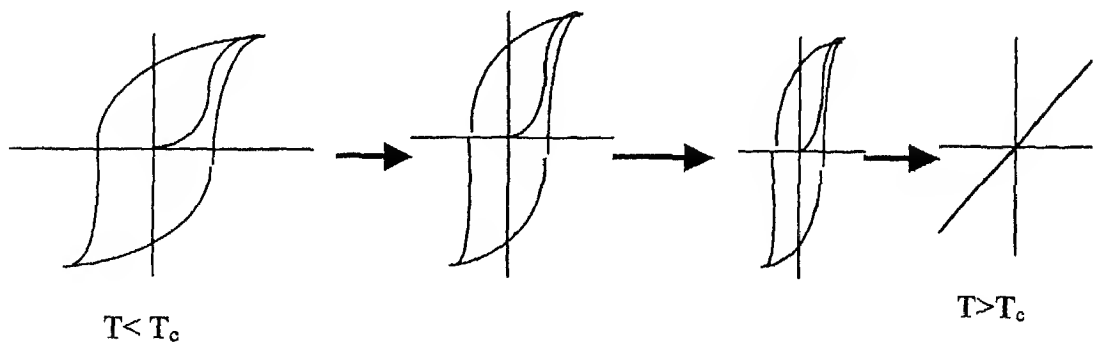


Fig. 1.6 Effect of temperature ( $T_c$ ) on nature of the hysteresis loop of ferroelectric thin films

Remnant polarization ( $P_r$ ) saturation polarization ( $P_s$ ) and coercive field ( $E_c$ ) values change with change in the temperature. At low temperature the thermal activation for randomization of domains is low and the width of hysteresis loop is large. On increasing the temperature the coercive field ( $E_c$ ) decreases and a narrower hysteresis loop results. On increasing the temperature beyond the  $T_c$  ( $T > T_c$ ) the hysteresis loop disappears and the material becomes paraelectric.

## 1.5 Applications of ferroelectric PZT materials in device technology

1. Ferroelectric PZT thin films because of their excellent piezoelectric properties are used in various applications like microphones, phonographs, transducers, actuators, particularly in microelectromechanical devices (MEMS).

2. In the ferroelectric materials the polarization state can be switched between two distinct polarization states which can be represented by corresponding binary states (0 and 1) used in digital electronics. Since the polarization remains after removal of electrical field, so the device can be utilized for non-volatile memory application. PZT devices show high switching speed and low switching power. They also have good radiation tolerance.

3. Capacitance of a parallel plate capacitor is given by

$$C = \frac{Q}{V} = \frac{\epsilon_0 \epsilon_r A}{d}$$

where  $\epsilon_r$  = permittivity of free space  
 $A$  = area of the plates  
 $Q$  = charge on each plate  
 $d$  = distance between two plates

If the thin PZT film is deposited on a conducting surface e.g. platinum-coated Si and another conducting layer (e.g. Pt) is deposited on it to act as the top plate of capacitor, a

PZT filled parallel plate capacitor device is produced Domains in PZT align along the field and produce a field opposite the applied field as a result a reduction in the over all potential (V) across the two plates takes place and the capacitance increased

$$C = \frac{Q}{V} = \frac{\epsilon_0 \epsilon A}{d}$$

$$C \propto \frac{1}{V}$$

Here  $\epsilon$  is the relative permittivity or dielectric constant of PZT

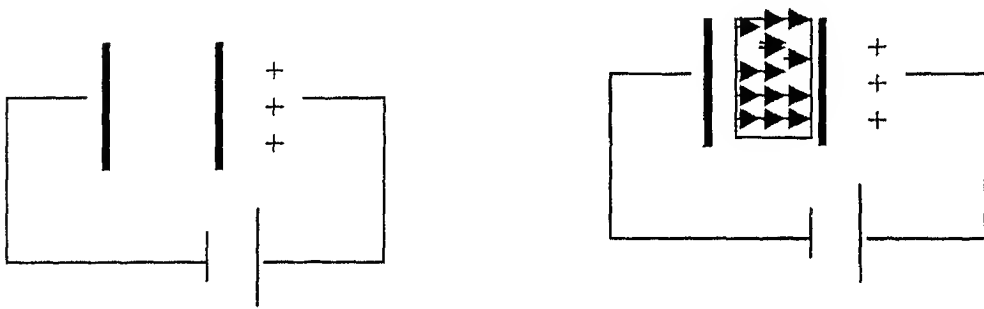


Fig 1 7(a) Capacitor without dielectric materials  
(b) Capacitor with ferroelectric materials

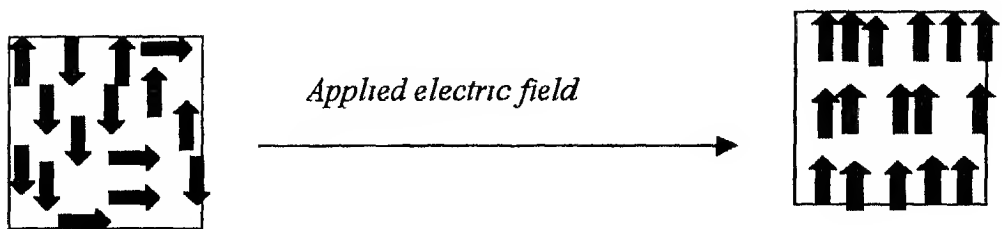


Fig 1 8 Effect of electric field on ferroelectric domain wall

4 For high density memory storage devices high capacitance is required so as to reduce the size of the individual storage capacitors For this purpose high dielectric constant materials are required High polarization of dipoles molecules creates large internal electric field which reduces the external field ( $C \propto 1/V$ ) Due to the ability of storing more charges the area can be reduced which allows more packing density of capacitors within a small substrate PZT with it high dielectric constant is a candidate material for ferroelectric random access memory

## 1.6 Ferroelectric thick films

Much of the research on PZT films has been conducted on thin films ( $\sim 0.2 \mu\text{m}$ ) primarily for non volatile memory application However for application in micro actuators pressure sensors and other micro-electromechanical devices much thicker films up to  $10 \mu\text{m}$  or thicker are needed Techniques such as CVD sputtering and sol gel have low deposition rate and are not suitable in their present form for preparation of thick films By the sol gel method for example the thickness of the film deposited by single step is  $< 0.1 \mu\text{m}$  and several coatings are required to get a thickness of even  $10 \mu\text{m}$  Efforts to increase the thickness by a single coating by increasing the sol concentration leads to cracking of the film Cracks arise due to differences in thermal expansion coefficients of substrate and deposited film Film sticks to the substrate and is not able to shrink in the direction parallel to substrate surface during annealing As a result high stress (tensile) develops in the film, which causes crack formation In case of sol gel films the films as prepared are highly porous Their densification during heat treatment leads to generation of stress which eventually causes crack formation In the following we first describe the effect of the thickness on the properties of PZT films This

is followed by a description of the various techniques for the preparation of the PZT films

### 1 6 1 Effect of thickness on properties of PZT films

#### 1 6 1 1 Effect thickness on ferroelectric properties

Properties of PZT and other ferroelectric films depend strongly on the film thickness. This appears to be primarily related to the variation in the strain in the film with thickness. Increased thickness leads to better phase formation as revealed by sharper x ray peaks and more homogenous microstructure. Several investigators have studied the dependence of electrical properties of PZT films on thickness [17-20].

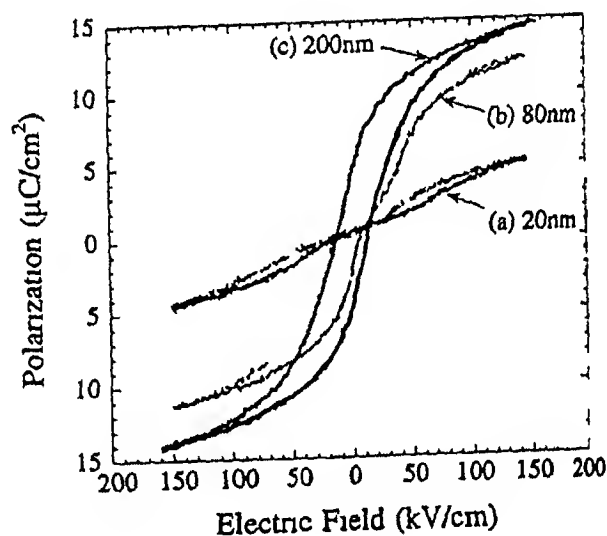


Fig 1.9 Effect of thickness on hysteresis loop i.e. saturation polarization and remnant polarization [17]



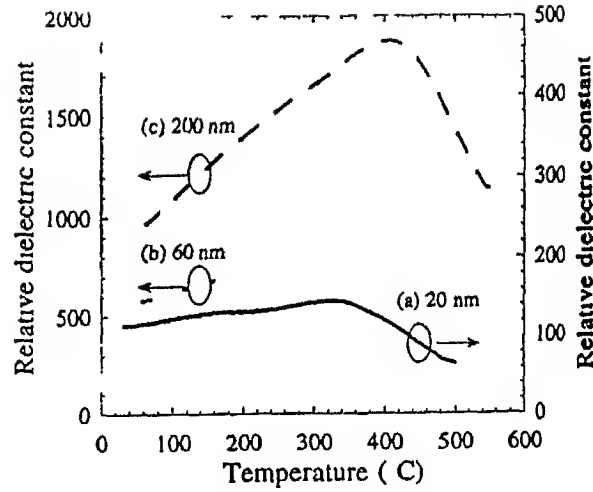


Fig 1.10 Plot between relative dielectric constant vs temperature for different thickness [17]

Fig (1.9) shows the change in hysteresis loop with thickness [17]. With increases in the thickness the loop becomes fills and approaches saturation showing higher remnant polarization  $P_r$  and saturation polarization  $P_s$ . The dielectric constant of the PZT films also increases with increased the thickness [17]. This has been attributed to the presence of an interfacial layer at the film electrode interface with a low dielectric constant [K Amanuma et al (18)]. Thus the measured capacitance is the series combination of two layers

$$\frac{1}{C_{Measured}} = \frac{1}{C_{Low}} + \frac{1}{C_{High}}$$

If  $d_{high}$ ,  $d_{low}$  and  $\epsilon_{high}$ ,  $\epsilon_{low}$  are the thickness and the dielectric constant of the two layer then

$$\frac{1}{C_{Measured}} = \frac{d_{High}}{\epsilon_0 \epsilon_{High} A} + \frac{d_{Low}}{\epsilon_0 \epsilon_{Low} A}$$

where A is the area of the top electrode. Using  $d = d_{Low} + d_{High}$  one gets

$$\frac{1}{C_{Measured}} = \frac{d}{\epsilon_0 \epsilon_{Hgh} A} + \frac{d_{Low}}{\epsilon_0 A} \left( \frac{1}{C_L} - \frac{1}{C_{Hgh}} \right)$$

Thus the measured capacitance and so the dielectric constant is reduced. The relative contribution of low dielectric constant layer decreases as the film thickness increases. Effect of thickness on ferroelectric properties of PZT [Pt/Pb(Zr<sub>0.53</sub> Ti<sub>0.47</sub>)O<sub>3</sub> / Pt/Ti/SiO<sub>2</sub>/Si] has been studied by R. Kurchania *et al* [4]. Hysteresis loop for thin film (0.25  $\mu$ m) is broad inclined and has a significant internal bias field in the positive direction. As the thickness increases the loop becomes squarer and more saturated. At constant applied field of 150 kV cm<sup>-1</sup> remnant polarization decreases progressively from 35 to 17  $\mu$ C cm<sup>-2</sup> on decreasing the thickness from 1.0 to 0.25  $\mu$ m [Fig. 1.11 and 1.12].

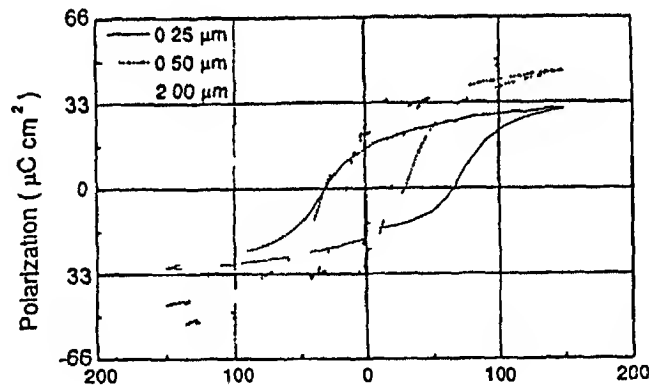


Fig. 1.11 Applied electric field vs polarization for different thickness (0.25, 0.50, 2.0  $\mu$ m) [4]

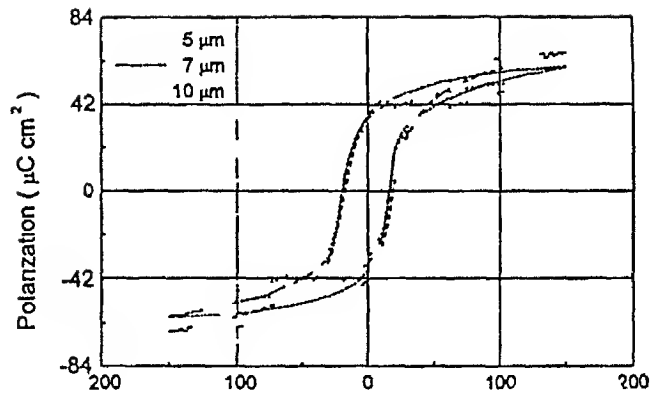


Fig 1 12 Applied electrical field vs polarization for different thickness (5 7 10  $\mu$  m)[4]

Beyond 2  $\mu$  m there is no further change in the nature of the loop though the values of  $P_r$   $P_s$  increases slightly [Fig 1 12]

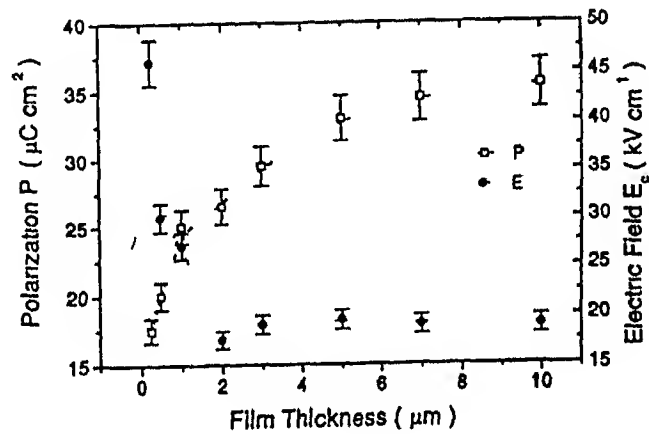


Fig 1 13 (a) Polarization ( $P_r$ ) and coercive field ( $E_c$ ) vs film thickness

(b) Film thickness vs saturation polarization [4]

The value of the coercive field was found to be almost constant ( $18$  to  $19 \text{ KVcm}^{-1}$ ) for thickness between  $2$  to  $10 \mu\text{m}$  and the increased sharply below  $2 \mu\text{m}$  reaching  $46 \text{ KVcm}^{-1}$  for  $0.25 \mu\text{m}$ . Abrupt change in  $E_c$  denotes a change in the switching behaviors at thickness below  $1.0 \mu\text{m}$ . The values obtained for the various parameters in sol gel thick films are found to depend significantly on the specific route used. Thus for acetic acid sol gel route as different from the propanediol route used by Kurchama et al [4] the coercive field changed little with thickness. It varied between  $30$ – $32 \text{ KV cm}^{-1}$  for all films in thickness range  $0.6$ – $12 \mu\text{m}$  with the remnant polarization increasing from  $17 \mu\text{C cm}^{-2}$  for a  $0.5 \mu\text{m}$  sample to nearly constant value of  $\sim 27 \mu\text{C cm}^{-2}$  for thickness  $\geq 3 \mu\text{m}$ .

### 1.6.1.2 Effect of thickness on C-V characteristics

Effect of thickness on C-V (capacitance vs applied voltage) curve has been studied by Sung Gap Lee *et al* [19]. They concluded that switching voltage decrease with increase in the number of coatings due to diminishing of stress at the film electrode interface.

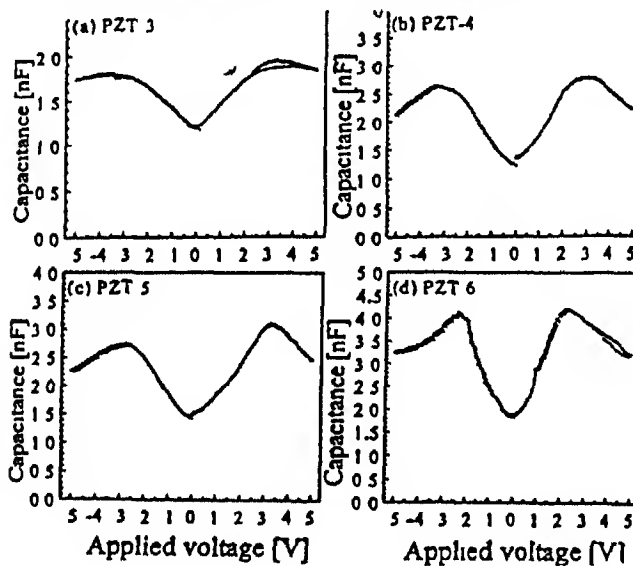


Fig 1.14 C-V characteristics of PZT hetero layers films [19]

### 1 6 1 3 Thickness dependent leakage current density

Current –density electrical field characteristic has been investigated on Pb (Zr<sub>0.53</sub>Ti<sub>0.47</sub>)O<sub>3</sub> film prepared by sputtering. Effect of thickness of the PZT film on leakage current density has been studied by T K Kundu et al [20] in the range between 70 to 680 nm thickness. This thickness range is important because it is useful for very large scale integration (VLSI). Different mechanisms dominate in different ranges of thickness. Leakage current density has been plotted as a function of electrical field. For thickness greater than 70 to 680 nm, various types of  $\log (J) \log (E)$  curves have been reported. For thickness more than 280 nm,  $\log (J)$ - $\log (E)$  behavior has been explained on the basis of GBLC (grain boundary limited conduction) mechanism. GBLC mechanism is generally observed in heterogeneous ferroelectric materials where resistivity of the grain boundary is much higher than that of the grain. Grain boundary potential energy ( $\phi_B$ ) dependent on grain boundary trap density ( $\eta_B$ )

$$\phi_B = \frac{e^2 \eta_B^2}{2 \epsilon_0 \epsilon_r N}$$

$\eta_B$  = grain boundary trap density

$\epsilon_0$  = permittivity of free space

N = dopant concentration

The relative permittivity,  $\epsilon_r$ , decreases with increase in the electrical field until polarization reaches saturation, therefore the barrier potential energy also increases with increases the field. As a result there is a reduction of  $\log (J) \log (E)$  slope.

For thickness less than 280 nm, trap control mechanism is dominating. This type of mechanism generally appears in quasi homogeneous thin films. Grain size and dielectric

constant remain constant in this thickness range J E characteristic shows Ohmic behavior at low electrical field ( $\cong 200KV/cm$ ) and large increase in the current density at high field range Sharp increase in conduction current over small voltage range has been explained in terms of cross over voltage ( $V_x$ )

$$V_x = \left( \frac{eN_t L^2}{\xi} \right) e^{\frac{E - E_{F0}}{k_B T}}$$

where  $E_t < E_{F0}$

$E_t$  = single trap energy level

$E_{F0}$  = equilibrium fermi level

$L$  = thickness of the films

$\xi_r$  = relative dielectric constant

$N_t$  = total concentration of traps

Grain boundaries do not show any significant effect on J E properties

#### 1 6 1 4 I-V Characteristics of thick films

Leakage current decreases with increase in the films thickness The leakage current is inversely proportional to  $d^3$  ( $d$ =thickness of film) K Amanuma *et al*[18] explained the behavior of leakage current with thickness by using Child s law Space charge limited current dominates the leakage current

$$I = \text{Constant} \left( \frac{V^2}{d^3} \right)$$

$I$  = current

$V$  = applied voltage and  $d$ =thickness of film

Leakage current decreases with increase in the films thickness On the other hand leakage current increases with increase in the applied voltage

## 1 6 2 Processing of thick films

### 1 6 2 1 Screen-printing

Screen printing method has been reported by Futakuchi et al (10) Pyroelectric thick films of composition  $0.92 \text{ PbZrO}_3 - 0.03 \text{ PbTiO}_3 - 0.05 [\text{Pb} (\text{Zn}_{1/3} \text{Nb}_{2/3}) \text{O}_3]$  (PZTZN) of 10–30  $\mu\text{m}$  thickness have been prepared. Powders of  $\text{PbO}$ ,  $\text{TiO}_2$ ,  $\text{ZrO}_2$ ,  $\text{Nb}_2\text{O}_5$  and  $\text{ZnO}_2$  were used as starting materials. First  $\text{ZnNbO}_6$  with columbite structure was prepared by pre calcinations at  $1000^\circ\text{C}$  for 2 hr. After that  $\text{ZnNbO}_6$ ,  $\text{PbO}$ ,  $\text{TiO}_2$  and  $\text{ZrO}_2$  powders were mixed in an appropriate ratio. Post calcination at  $900^\circ\text{C}$  for 2 hr was done in a magnesia covered crucible. The calcinated product was crushed and then ground by planetary ball milling for 3 hr. The size of the ground powders was between 0.4 to 2  $\mu\text{m}$ . The screen printable paste was prepared by mixing ethyl cellulose and  $\alpha$  terpineol with ground powders (PZTZN) in three roller mill. After screen printing of PZTZN paste by a 200 mesh screen mask on an appropriate substrate it is allowed to level for 10 min and dried at  $120^\circ\text{C}$  for 10 min. Before sintering the organic binder is burnt out at  $600^\circ\text{C}$  for 10 min. The firing of thick films has been done in magnesia covered crucible over a temperature range  $1100^\circ\text{C}$  to  $1200^\circ\text{C}$  for 2 hr. The thickness of PZTZN film after sintering was  $\sim 25 \mu\text{m}$ .

$\text{Pb}(\text{Zr-Ti})\text{O}_3$   $\text{Pb}(\text{Zn-Nb})\text{O}_3$  thick film has also been prepared by a low temperature firing processing employing oxide powders and a glass ceramic [T Kubota et al (12)]. Powder of  $0.7 \text{ Pb}(\text{Zr-Ti})\text{O}_3 - 0.3 \text{ Pb}(\text{Zn-Nb})\text{O}_3$  was obtained by mixing and calcination the powders of  $\text{Pb}_3\text{O}_4$ ,  $\text{Zn-NbO}_6$  and  $\text{BaTiO}_3$ . Small amounts of precursor  $\text{BaTiO}_3$  were added to stabilize the single perovskite phase during the firing processing. The  $\text{Pb}(\text{ZrTi})\text{O}_3$  and  $\text{Pb}(\text{ZnNb})\text{O}_3$  powders were mixed in appropriate ratios and calcined at  $950^\circ\text{C}$  for 5 hrs.

Glass ceramic of  $\text{PbO-TiO}_2\text{-ZrO}_2\text{-SiO}_2\text{-B}_2\text{O}_3$  containing nucleation initiators of  $\text{TiO}_2$ ,  $\text{ZrO}_2$  were used. Crystallization of the glass ceramic studied separately was initiated at  $540^\circ\text{C}$  and  $\text{Pb}(\text{ZrTi})\text{O}_3$  perovskite phase was formed near  $670^\circ\text{C}$ . Necking among the glass ceramic particles was observed at  $750^\circ\text{C}$ . The paste for thick film was prepared by mixing of  $0.7 \text{ Pb}(\text{Zr-Ti})\text{O}_3$   $0.3 \text{ Pb}(\text{Zn-Nb})\text{O}_3$  powder, lead based glass ceramic and organic vehicle (ethyl cellulose,  $\alpha$ -terpineol). This paste was printed on substrate (Pt coated  $\text{ZrO}_2$  substrate) and dried at  $150^\circ\text{C}$  for 10 min and fired at  $800^\circ\text{C}$ – $950^\circ\text{C}$  for 3 hr. The thickness of fired film was reported to be  $50 \mu\text{m}$ .

### **1.6.2.2 Thick PZT glass film composite by plasma spray method**

Thick films of PZT have been prepared by a plasma spray process by Sherril et al [11]. Powder mixture of PZT and an aluminosilicate glass with particle size of 1 to  $3 \mu\text{m}$  was used. The powders were plasma sprayed on to stainless steel substrate. The film thickness ranged from 0.08 mm to 0.25 mm. The dielectric constant of the film varied between 58 and 20 with dissipation factor between 0.019 to 0.032.

### **1.6.2.3 PZT thick film by aerosol deposition method (ADM)**

PZT film of  $10 \mu\text{m}$  thickness has been reported by Jun-Akedo et al [13] using aerosol deposition method (ADM). Aerosol deposition method (ADM) is a kind of gas deposition method (GDM) without vaporization of the material. In GDM, individual particles of ceramic material with diameter of approximately  $0.1 \mu\text{m}$  are mixed with carrier gas (He gas was used as carrier gas) to form a colloidal aerosol flow. The colloidal aerosol was ejected through the micro orifice nozzle and deposited on to substrate. The collision of the ultra fine particle (UFP) with the substrate converts a part of its kinetic energy to local thermal energy which promotes the bonding between the substrate and amongst the ultra



fine particles. In aerosol deposition method, the pressure in aerosol chamber was about 480 torr and that in the deposition chamber was 0.5 to 1.0 torr. The nozzle has an orifice size of 5mm x 300mm. The relative velocity of nozzle along the substrate was 0.125 to 1.25mm/s and distance between the nozzle and substrate was 2.5mm to 10 mm.

Schroth et al [14] deposited thick PZT layers by gas deposition method using ultra fine particles with subsonic gas jet stream. A sintered ceramic layer formed on the substrate. By scanning the nozzle over the substrate repeatedly, thickness of 100  $\mu$ m was reported. A damage layer forms at the interface between the PZT and the Si substrate. The remnant polarization and coercive field improved on annealing the film, mainly due to the crystal growth of small crystallites.

#### **1.6.2.4 Thick film by electrophoretic deposition**

Thick film of PZT has been prepared by electrophoresis from suspension of commercially available PZT powder suspended in acetone with addition of nitric acid and nitrocellulose. Films up to 32  $\mu$ m thick have been reported by Sweeney T. et al [15] by using electrophoresis deposition, multi coating and sintering method.

#### **1.6.2.5 Thick film by interfacial polymerization**

PZT thick film of 20  $\mu$ m has been reported by Yamane *et al*[16] by interfacial polymerization using metal organic precursor. Commercially available PZT precursor solution was diluted with hexane containing acetyl acetone as a chelating agent. The solution was poured on water contained in a teflon reaction container of 88 mm inside diameter. A translucent gel film was formed at the interface of the two immiscible liquids which floats on water. It shrank as the evaporation of solvent proceeded until its

diameter decreased to about 45% of its initial value. The dried gel film was almost pore free and its thickness was reported to be  $10\text{ }\mu\text{m}$ .

### **1.6.3 PZT thick film by sol-gel**

#### **1.6.3.1 The sol-gel process**

In sol gel processing inorganic oxides and glasses are prepared by a wet chemical method. Sol gel method is generally preferred for thin film preparation because of its unique advantages over other methods. The sol-gel has the following advantages:

1. Dopants can be easily introduced for desired electrical and physical properties.
2. Good composition homogeneity is obtained.
3. Processing is carried out at low temperature.
4. Thickness of the films can be controlled by modifying the sol concentration and varying the number of coatings.

However, it has some disadvantages also:

1. Long processing time.
2. Residual fine pore after drying and annealing.
3. Large shrinkages in films during heating and annealing which cause crack formation in films.

Two types of sol gel processing are generally used:

##### **(1) Colloidal processing**

In this, a suspension of fine particles of size  $1\text{--}1000\text{ nm}$  is used. Particles form the gel network and subsequently sinter to yield a continuous film.

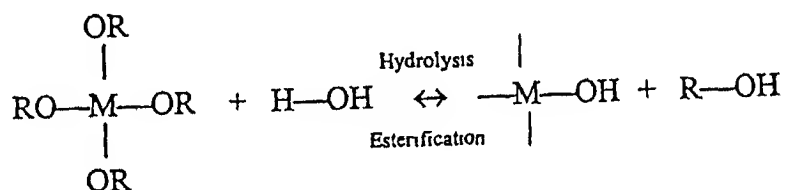
## (2) Polymeric processing

In this case different metal alkoxides are used as precursors. All metals are capable of forming an alkoxide  $M(OR)_x$  in which alkyl group is bonded to the metal by means of oxygen atoms. In the sol gel method  $M(OR)_x$  metal alkoxide is mixed with water and appropriate solvent (usually an alcohol). A small amount of acid and base is added to catalyze the reaction. To avoid or minimize the self condensation some metal salt like chloride, nitrates or acetate are also used. Alcohol, chloride, nitrates and acetate play an important role for determination of the thickness and volume shrinkage. During polymeric gel formation, hydrolysis and condensation reactions take place simultaneously.

### 1.6.3.1.1 Hydrolysis mechanism

Metal alkoxides and water are mixed together in common solvent which is usually an alcohol. A small amount of an acid or a base acts as a catalyst. Two types of reactions, hydrolysis and condensation reactions, take place simultaneously.

#### (1) Hydrolysis



#### (2) Condensation

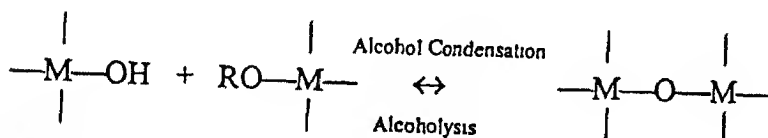
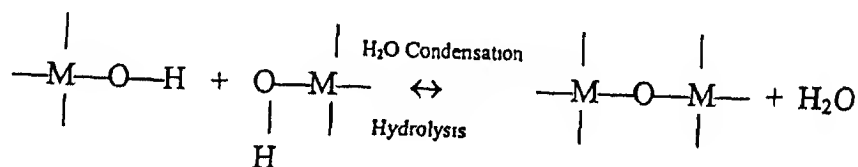


Fig 1.15 hydrolysis and condensation reaction 21

## Acid-catalyzed hydrolysis

In this mechanism lone pair electron of oxygen of water attack on metal part ( $Zr^{+4}/ Ti^{+4}$ ) of alkoxide called electrophilic reaction. Partially hydrolyzed tetrahedral product results without inversion in configuration. In acid catalyzed reaction substitution of one OR group of alkoxide with OH group takes place.

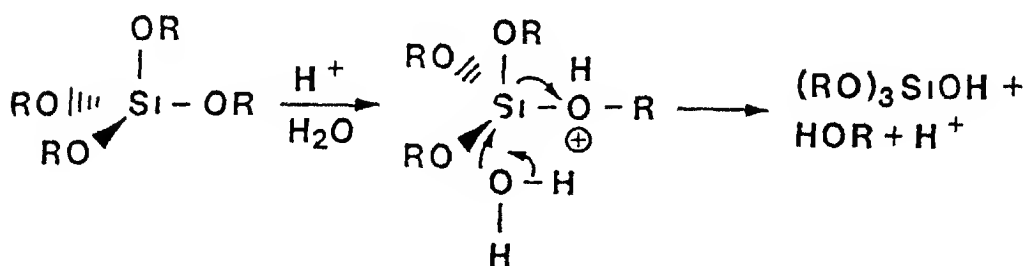


Fig 1.16 Acid catalyzed hydrolysis mechanism

In acidic condition partially hydrolyzed monomers are produced which result in more linear and lightly cross linked network.

## Base-catalyzed hydrolysis mechanism

This mechanism dominates at high pH, called nucleophilic substitution reaction. In this mechanism, nucleophilic attack occurs on  $M^{+n}$  (metal) from opposite side of leaving group OR as a result tetrahedral inverted product is obtained.

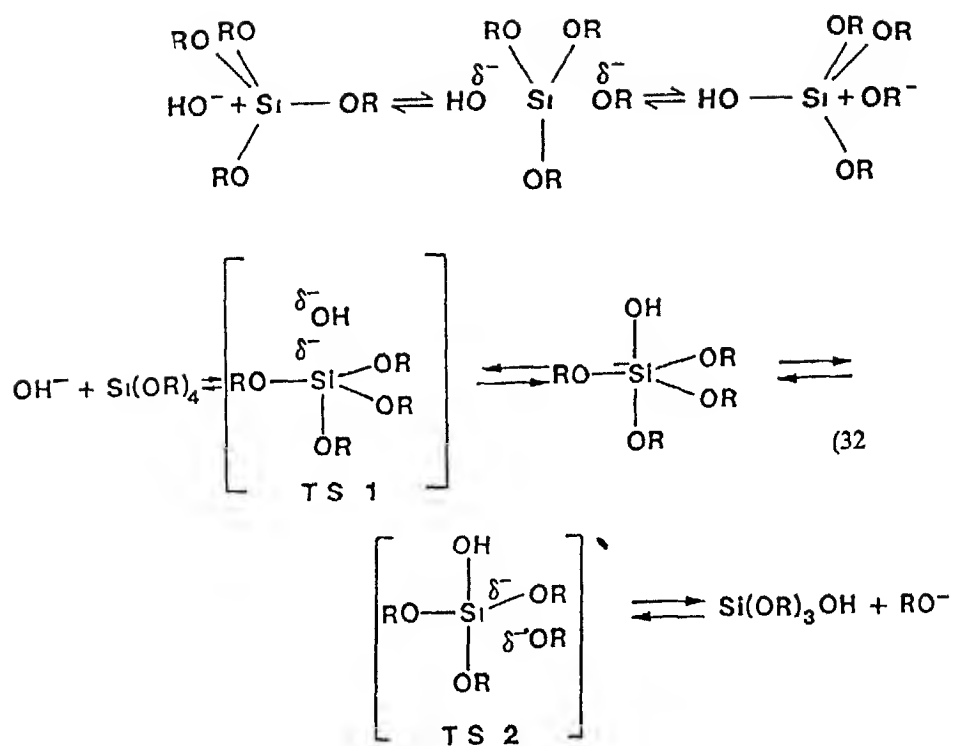


Fig 1 17 Base-catalyzed hydrolysis mechanism

### 1 6 3 1 2 Condensation mechanism

Gelation is the process in which the sol is transformed to 3-d network by elimination of water or some other group like alcohol. Both hydrolysis and condensation reaction occur simultaneously. The relative rate of both of these reactions depends on the experimental condition like solvent, water, alkoxide ratio, inductive effect, and type of chelating group. Water is a by product of the condensation reaction so that increased amount of water will lead to reverse reaction which inhibits the condensation reaction (Le Chatelier's principle). Amount of acid and basic medium (hydrolyzing agents) determine the mechanism of reaction and pore size structure of gel.

### 1 6 3 2 Sol-gel process for thick films

In the conventional film deposition by sol gel method the sol is deposited on the substrate by methods such as dip coating or spin coating. On drying and heating a dense film is obtained. The thickness of the film made by a single coating is less than  $0.1 \mu\text{m}$ . This cannot be increased much by increasing the sol concentration alone due to the formation of cracks in the thicker films. Several additives are used in the sol to avoid the crack formation by reducing the condensation so that the film can easily relax during shrinkage and the crack formation is avoided. Some of the methods are described below.

#### 1 6 3 2 1 Thick film by using diol and acetylacetonate

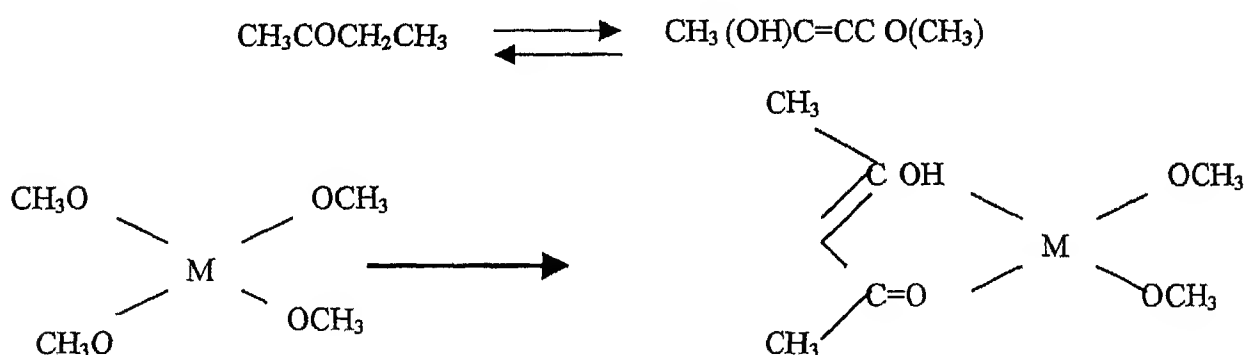


Fig 1 18 Role of chelating agent(Only two  $-\text{OCH}_3$  group takes part in hydrolysis reaction. Other two  $-\text{OCH}_3$  group are protected by acetylacetonate (chelating group)

Several diols like glycol, propandiol, butandiol and pentandiol have been used as solvent for  $\text{Pb}(\text{CH}_3\text{COOH})_2 \cdot 3\text{H}_2\text{O}$ . The diols act as gel forming agent during gelation because of their ability to link Zr and Ti monomers. Acetylacetonate also plays an important role during hydrolysis process. It acts as a chelating agent and controls the processes of

hydrolysis and condensation Acetylacetonate replace the two  $-\text{OC}_3\text{H}_7$  groups of  $\text{Zr}(\text{OC}_3\text{H}_7)_4$  and  $\text{Ti}(\text{OC}_3\text{H}_7)_4$  so these sites do not take part in the hydrolysis process Hydrolysis takes place only at the two remaining  $-\text{OC}_3\text{H}_7$  positions As a result limited and controlled hydrolysis takes place During condensation process only these two  $-\text{OH}$  groups take part As a result a more relaxed structure with reduced probability of highly stressed 3 d network is obtained Crack free thick films have been reported by using diol and acetylacetonate [2 5]

#### **1 6 3 2 2 Thick films by using tri-alkoxy-silanes**

Tri alkoxy silanes  $\text{CH}_3\text{CH}_2\text{M}(-\text{OR})_3$  have one non  $-\text{hydrolysable}$  group as a result it does not take part in condensation reaction and avoids the formation of highly stressed 3 d network structure Thick films of 0.6 to 5  $\mu\text{m}$  without cracks have been reported using the dip coating process [ F Del Monte *et-al* (6)]

#### **1 6 3 2 3 Thick films by using progressive (step wise) heating schedule**

Effect of progressive heating have been reported by J Koo et al [7] Uniform and crack free thick films have been reported by applying different heating schedules Due to slower and long heating thermal shock can be avoided and longer heating provides enough time to remove the organic and other residue PZT thick films of 8000  $\text{\AA}$  have been reported

#### **1 6 3 2 4 Thick films by using suitable substrate**

Most of the stresses are developed due to difference in thermal expansion coefficients of the substrate and the films during annealing process Alumina has comparable thermal expansion coefficient with PZT as a result nearly equal thermal expansion during heating (annealing) and shrinkage during cooling occur which inhibit the possibility of

stress in the film PZT films of thickness  $600\text{ }\mu\text{m}$  have been reported by A Schonecker et al [8] Thermal expansion coefficient of  $\text{ZrO}_2$  is comparable to silicon substrate A thin coating of  $\text{ZrO}_2$  over silicon substrate allows thick film to grow with reduced thermal stress in the film Microstructure and electrical properties have been improved by minimizing the stress developed in films using  $\text{ZrO}_2$  coating over substrate [K G Brooks et al (9)]

## **1 7 Statement of problem**

Several methods have been suggested to prepare thick film by sol gel processing In the present work a polymer Poly vinylpyrrolidone or (PVP) has been utilized to prepare thick films of PZT Hiromitsu Kozuka et al [25] used Poly (vinylpyrrolidone) for preparing crack free  $\text{BaTiO}_3$  films of thickness  $>1\text{ }\mu\text{m}$  by single dip coating The present work is aimed at exploring the use of PVP for making of thick PZT films It is the aim of work to show the effect of sol composition and other variables on the thickness and properties of PZT films



# Chapter 2

---

## Experimental Procedures

### 2.1 Introduction

Different types of substrates for film deposition have been reported in literature like MgO(100) single crystal, platinum, fused quartz, sapphire,  $\text{ZrO}_2$  and silicon. In the present work, Si(100) n-type has been used as substrate for film deposition. Si(100) has some advantages over other substrates. In the (100) plane, the silicon crystal has the least number of bonds so that a minimum of interface-charge density  $Q_f$  exists on the surface. Due to this minimum interface charge density, it is generally chosen for fabrication of MOS (metal oxide semiconductor) and metal-ferroelectric-semiconductor devices. Au/Pd /  $\text{Pb}_{1.05}(\text{Zr}_{0.53}\text{Tl}_{0.47})\text{O}_3$ /Au/Pd /  $\text{ZrO}_2$  / Si(100) n capacitor has been prepared in present work with PZT as the ferroelectric material.

PZT ferroelectric ceramic with composition  $\text{Pb}_{1.05}(\text{Zr}_{0.53}\text{Tl}_{0.47})\text{O}_3$  is deposited on Au/Pd coated  $\text{ZrO}_2$  / Si(100) substrate. Au/Pd coating on substrate acts as the bottom electrode for PZT ferroelectric capacitor. Au/Pd top electrode was deposited by sputtering  $\text{ZrO}_2$  coating over silicon substrate acts as the barrier for lead diffusion through interface. For

bottom and top electrode Pt was also attempted in place of Au Pd but non conductivity problem arises during heating The problem with Pt electrode has been discussed in next section The complete system Au Pd /  $\text{Pb}_{1.05}(\text{Zr}_{0.5} \text{Ti}_{0.47})\text{O}_3$  / Au Pd / ZrO<sub>2</sub> / Si (100) acts as a capacitor with ferroelectric material PZT and Au Pd act as a bottom and top electrode

## 2.2 Sample preparation

### 2.2.1 Silicon wafer cleaning

RCA cleaning is generally used to clean silicon wafer (Appendix 1)

In the present work silicon wafer was dipped in a mixture of HF and distilled water (50:1) for 20 min After 20 min silicon wafer was transferred to triple distilled water After washing with triple distilled water it was dried in open air and kept in a sealed plastic container

### 2.2.2 Deposition of ZrO<sub>2</sub> film over Si (100) substrate by spin coating

Yushi Shichi et al (24) reported that Pb (a constituent of PZT) oxygen and silicon diffuse through the interface of PZT film and silicon at the film annealing temperature (~650°C) Activated oxygen diffuses into interface and reacts with elemental silicon of substrate and produces SiO<sub>2</sub>



The resulting SiO<sub>2</sub> reacts with PbO to form Pb SiO<sub>3</sub>



$\text{Pb}_2\text{SiO}_4$  accelerate the diffusion of silicon into films. As a result, lead deficient PZT layer forms at the interface of the PZT film and the  $\text{Si}$  substrate, which causes degradation in dielectric constant and other properties.

Use of several materials such as  $\text{CeO}_2$ ,  $\text{MgO}$ ,  $\text{SrTiO}_3$  and  $\text{TiO}_2$  etc. as buffer layer between  $\text{Si}$  and PZT has been attempted. Zirconia ( $\text{ZrO}_2$ ) has been found to be effective in inhibiting the diffusion of Pb to the underlying  $\text{Si}$ . Horita et al (35) used a heteroepitaxial yttria stabilized Zirconia (YSZ)  $(\text{ZrO}_2)_{1-x}(\text{Y}_2\text{O}_3)_x$  film as a buffer layer. It has high chemical stability, high resistivity and large dielectric constant of about 30 and can be heteroepitaxially grown on  $\text{Si}$ . By making use of the fact that if the unit cell of the grown PZT (001) film and yttrium stabilized zirconia (YSZ) layer are rotated  $45^\circ$  from each other, the lattice mismatch is low (10.9 %). The authors were able to obtain plane oriented PZT film in which a 10 nm thick YSZ buffer layer was able to prevent the PZT film from reacting with the  $\text{Si}$  substrate. K.G. Brooks et al (9), M.I. Mealeto (21), N. Yu (22) and A. Mehnert (23) in their work deposited thick PZT films on well polished  $\text{ZrO}_2$  substrate and they concluded that the high thermal expansion of  $\text{ZrO}_2$  relative to  $\text{Si}$  (100) allows the deposition of thicker layer of PZT with reduced thermal stress. Electrical properties can be improved by minimizing the thermal stress (21–24).

Hence in present work, we have deposited a  $\text{ZrO}_2$  buffer layer on  $\text{Si}$  by a sol-gel method.

**Table 2 1** Specification of the chemicals used for sol preparation for  $\text{ZrO}_2$  coating

S No	Name of compound	Mol Wt	Density	Concentration	Product detail
1	Zr(n Propoxide)	327.57	1.05	0.5 M	Fluka chemika
2	Diethanol amine (DEA)	105.14	1.098	0.37M	S D Fine Chem
3	Isopropyl alcohol	60.10	1.245		S D Fine Chem
4	$\text{H}_2\text{O}$ (triple distilled)	18	1.0	0.9M	-

### 2.2.2.1 $\text{ZrO}_2$ sol preparation

For preparation of  $\text{ZrO}_2$  sol Zr(n propoxide) was taken as the Zr source. Diethanolamine (DEA) is used as a chelating agent and isopropyl alcohol as a solvent for DEA and Zr(n propoxide). DEA, 0.71 ml is mixed with 7.9 ml isopropyl alcohol in 50 ml beaker. This solution was stirred with the help of a magnetic stirrer for 30 min. Isopropyl alcohol (7.9 ml) and water (0.324 ml) are taken in another 50 ml beaker and stirred for 30 min. In the first mixture (solution of DEA and isopropyl alcohol) 3.1 ml of Zr(n Propoxide) is added drop by drop and mixing carried out for one hour. After complete mixing a clear solution of DEA, isopropyl alcohol and Zr (n Propoxide) is obtained. This solution is added to the solution of isopropyl alcohol and water drop by drop and stirring carried out for another one hour. After this a clear sol of  $\text{ZrO}_2$  is obtained. This sol is stored in an airtight plastic container. The specification of the chemicals used for sol preparation is given in Table 2.1. The details of the calculation for amounts of the various ingredients used are given in Appendix 2. The flow chart of sol preparation is given in fig2.1.

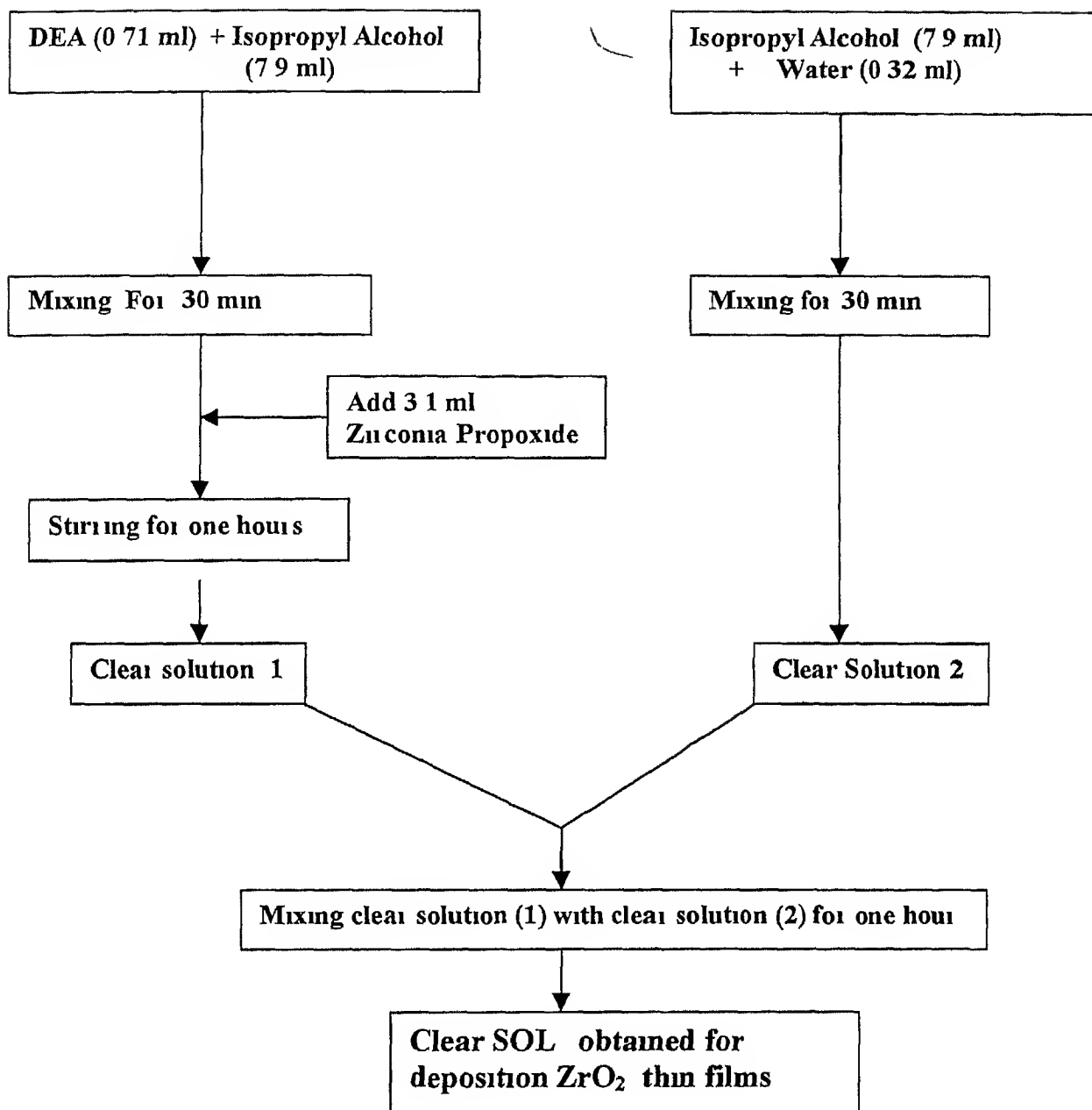


**Fig 2.1 Flow chart diagram for ZrO<sub>2</sub> Sol preparation**

### **2 2 2 2 Deposition of $\text{ZrO}_2$ film**

Spin coating method has been utilized to deposit thin films of  $\text{ZrO}_2$  on  $\text{Si}$  substrate. The speed (RPM) of spinning and concentration of the sol are two important factors in determining the thickness of the film. The viscosity of the sol is also an important factor in controlling the thickness of the film. Thickness of the film is inversely proportional to rotational velocity of spinner. The rotational speed of spinner was kept constant at 2000 RPM during the spin coating. After deposition, the film is heated at  $400^\circ\text{C}$  for 5 min in a furnace in air. Only one coating of  $\text{ZrO}_2$  was deposited on silicon substrate.

### **2 2 3 Deposition of Au-Pd bottom electrode on $\text{ZrO}_2/\text{Si}$ (100) by sputtering**

An attempt was first made to deposit a Pt bottom electrode by using a Pt target fabricated in laboratory. However, after the heat treatment during the multiple coating deposition, the Pt layer was found to become non-conducting. Hence, it was decided to use a layer of Au-Pd as bottom electrode because the target for this was available in the laboratory. In present work, Au-Pd thin layer was deposited on  $\text{ZrO}_2/\text{Si}(100)$  substrate by sputtering using HUMMER(5 A) sputtering system (Anatech Ltd).

For sputtering, following conditions were used

Vacuum in sputtering chamber = 80 millitorr

Plasma discharge current = 10 milli ampere

Voltage control setting = 3.4

Total time for sputtering = 10 min

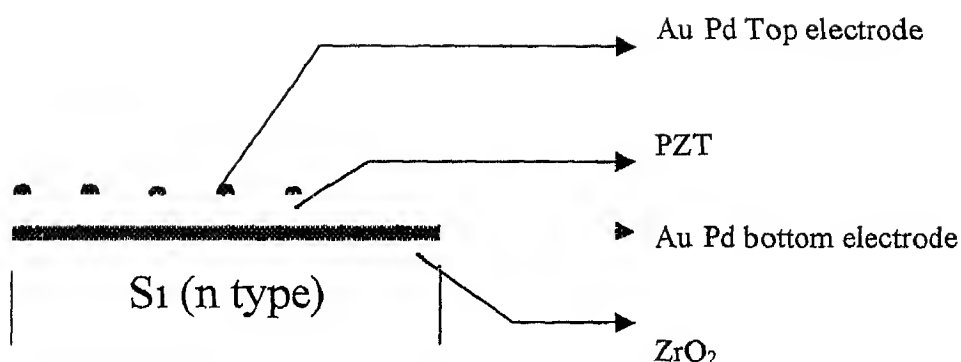


Fig 2 2 Schematic of the Au Pd/PZT/Au Pd/ZrO<sub>2</sub>/ Si(100) sample

The film was found to have a low resistance when checked by a multi meter The conductivity did not changed after deposition of the film

#### 2 2 4 Deposition of PZT films on Au-Pd /ZrO<sub>2</sub> /Si (100) substrate by spin coating

Thick films are useful for several important applications The main problem in thick film preparation by sol gel is the generation of cracks in the films due to the tensile stress produced during film densification and annealing During annealing the film sticks to the substrate and is not able to shrink in the direction parallel to the substrate due to constrain of the substrate As a result high tensile stress ( $\cong 100$  MPa) appears in the films which causes crack formation in the films [Hiromitsu Kozuka et al (25)]

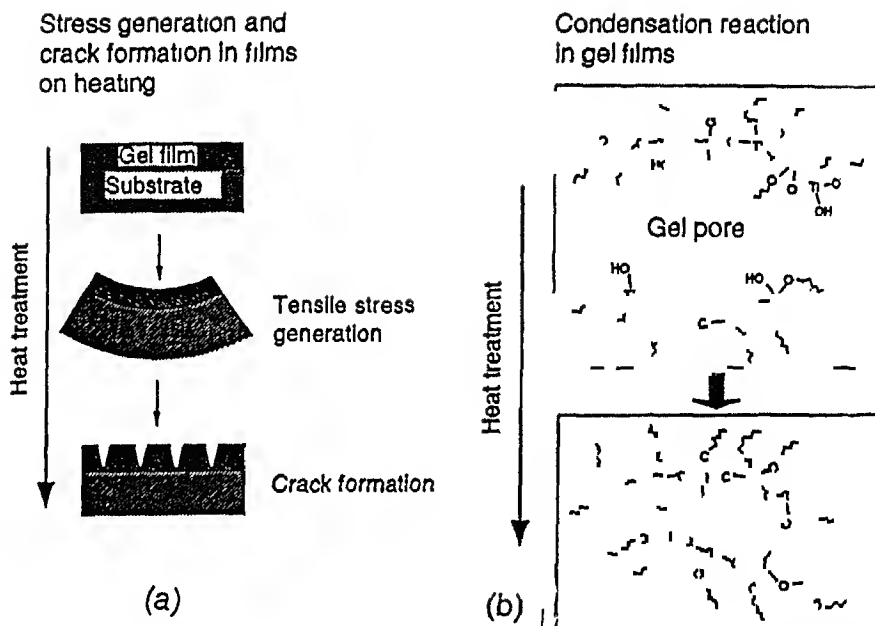


Fig 2.3 (a) Tensile stress evolution and crack formation in gel under heat treatment  
 (b) Condensation and pore collapse in gel films under heat treatment  
 [H Kozuka and M Kajimura (25)]

Condensation reaction plays a major role in crack formation process in the sol gel derived film. By minimizing the condensation reaction, the stress developed in the film can be minimized and crack free film can be grown. In our present work, to minimize the condensation reaction in the gel, an organic polymer with amide group namely (PVP) poly (vinylpyrrolidone) of mol wt 40000 has been introduced in sol during preparation of the PZT.

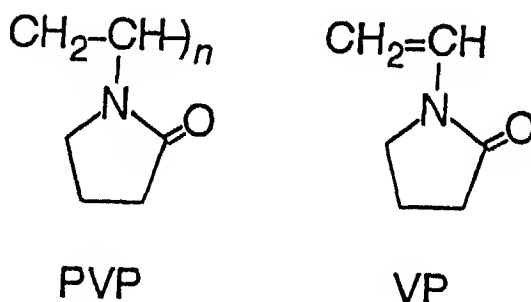


Fig 2.4 Poly (vinylpyrrolidone) PVP and N vinyl 2 pyrrolidone (VP) [25]



PVP with carbonyl group acts as a protecting group for  $-OH$  group of metalloxane polymer by forming strong hydrogen bond between carbonyl group of PVP and  $-OH$  group of metalloxane. Due to strong hydrogen bonding the condensation reactions are suppressed. As a result more structural relaxation can occur in the films at high temperatures. Due to capping of metalloxane polymer with carbonyl group of PVP high density thick films of  $BaTiO_3$  without cracks have been prepared by single dip coating (25)

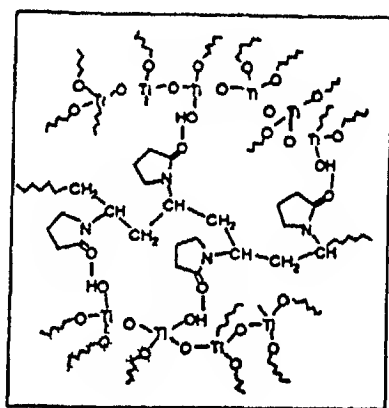


Fig 2.5 PVP inhibiting the condensation reaction in gel films by protecting the  $-OH$  group by carbonyl group PVP [25]

## 2.2.4.1 Preparation of PZT sol

The details of the chemicals used to prepare the PZT sol of desired compositions are given in table 2.2. A flow chart for the sol preparation is given in figure (2.5). The calculations of the amount of the various ingredients are given in Appendix 3.

**Table 2 2** Chemical used for  $\text{Pb}_{1.05}(\text{Zr}_{0.535}\text{Ti}_{0.465})\text{O}_3$  sol preparation

S N	Name of the compound	Mol Wt	Density	Yield (%)	Source
1	$\text{Pb}(\text{CH}_3\text{COO})_2 \cdot 3\text{H}_2\text{O}$	379.33	2.55	99.70	E Merck
2	Zr(n Propoxide)	327.58	1.05	74.88	Fluka
3	Ti(n Propoxide)	340.35	0.995	99.99	Alfa
4	$\text{CH}_3\text{COOH}$	60.00	1.045		NICE
5	Isopropanol	60.10	1.43		NICE
6	PVP(polyvinylpyrrolidone)	111.0(monomer) Polymer (40000)			SRL (Sisco Research Lab)

**Table 2 3** Amount of PVP for PZT with different PVP(monomer)/Ti molar ratio

S No	Sample No	Amount of PVP(gm) for different PVP/Ti ratio
1	PZT (no PVP)	0.00
2	PZT (PVP/Ti=0.2)	0.103
3	PZT (PVP/Ti=0.5)	0.25
4	PZT (PVP/Ti=1.0)	0.516
5	PZT (PVP/Ti=1.5)	0.774
6	PZT (PVP/Ti=2.0)	1.032

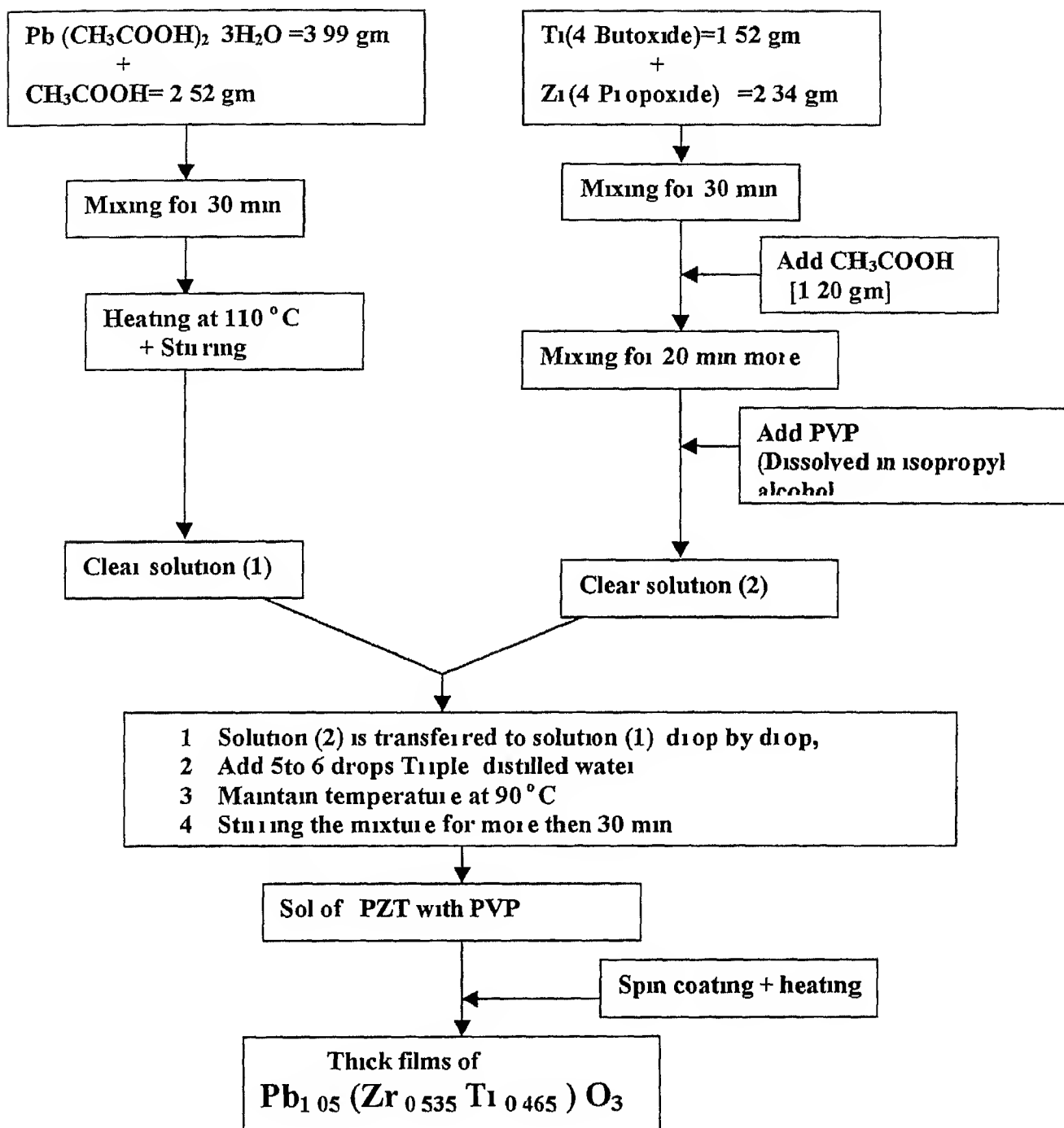


Fig 2.6 Flow chart for sol preparation of  $\text{Pb}_{1.05}(\text{Zr}_{0.535}\text{Ti}_{0.465})\text{O}_3$  with PVP

Typically for the preparation of a sol with PVP/Ti ratio 1:1 the following procedure was used. Titanium butoxide 1.582 gm (yield 99.9%) was weighed in a 50 ml beaker inside a glove box in dry air (RH 30%). In this beaker 2.34 gm of zirconia propoxide (yield 74.88%) is also weighed. This mixture is stirred for 30 min with the help of a magnetic stirrer. To this was added 1.20 gm of acetic acid drop by drop. PVP (0.516 gm) was taken in a beaker and to it was added isopropanol and the mixture stirred. The amount of isopropanol is just sufficient to obtain a clear solution of PVP. This PVP solution was added drop by drop to the alkoxide mixture and the resulting solution was allowed to mix for 30 min. In a glove box 3.99 gm of lead acetate was taken in a three-necked flask (the lead acetate was not analyzed for additional moisture absorption so there may be uncertainty in composition). Acetic acid of 2.52 gm was added to lead acetate. The three-necked flask with mixture of lead acetate and acetic acid was heated in an oil bath and the temperature was maintained at 90°C for 30 min with constant stirring. The alkoxide solution was then added to lead acetate solution drop by drop at temperature 90°C and also 5 to 6 drops of triple distilled water were added during mixing. This mixing process was continued for another 30 to 40 min until a clear sol obtained. This clear sol is cooled to room temperature. After completion of this process volume of sol obtained was 12 to 15 ml. A solution of isopropanol and acetic acid mixed in equal volume is prepared and this is used to bring up the volume of the sol to 16 ml. This gives a sol of concentration of 0.63 M. A part of this was further diluted to the 0.315 M by adding equal volume of isopropanol acetic acid mixture. Both the sols were stored in sealed plastic container. The various steps in device preparation are illustrated in fig2.7

## 2.2.4.2 PZT thick film deposition

Sol of  $\text{Pb}_{1.05}(\text{Zr}_{0.53}\text{Ti}_{0.46})\text{O}_3$  has been deposited on Au Pd/ZrO<sub>2</sub>/Si(100) by spin coating. It has been reported that thickness of the film depends on the following factors

- (1) Ratio of titanium propoxide and PVP
- (2) Molecular wt of PVP polymer. Higher the molecular weight of polymer, more thickness of the films can be grown without cracks.

During spin coating, the rotational speed of spinner was kept constant at 2000 RPM. For deposition, only one drop of PZT sol has been used in single step and then coated PZT film substrate is heated at 400°C for 5 min in presence of air. This process is repeated several times according to requirement of thickness. After every coating and drying at 400°C, film surface was observed to check its microstructure and presence of cracks by using optical microscope at 100 magnification. In the present work, 12 to 15 coatings have been deposited and no cracks were found. After getting desired thickness, the film was annealed at 650°C for 40 min in the presence of air to get appropriate morphology. After annealing at 650°C, Au Pd top electrode was deposited on PZT films by sputtering using a mask. After deposition of Au Pd top electrode, the film is heated to 400°C for 5 min. The sandwiched PZT layer (ferroelectric) between bottom and top Au Pd electrode acts as capacitor.

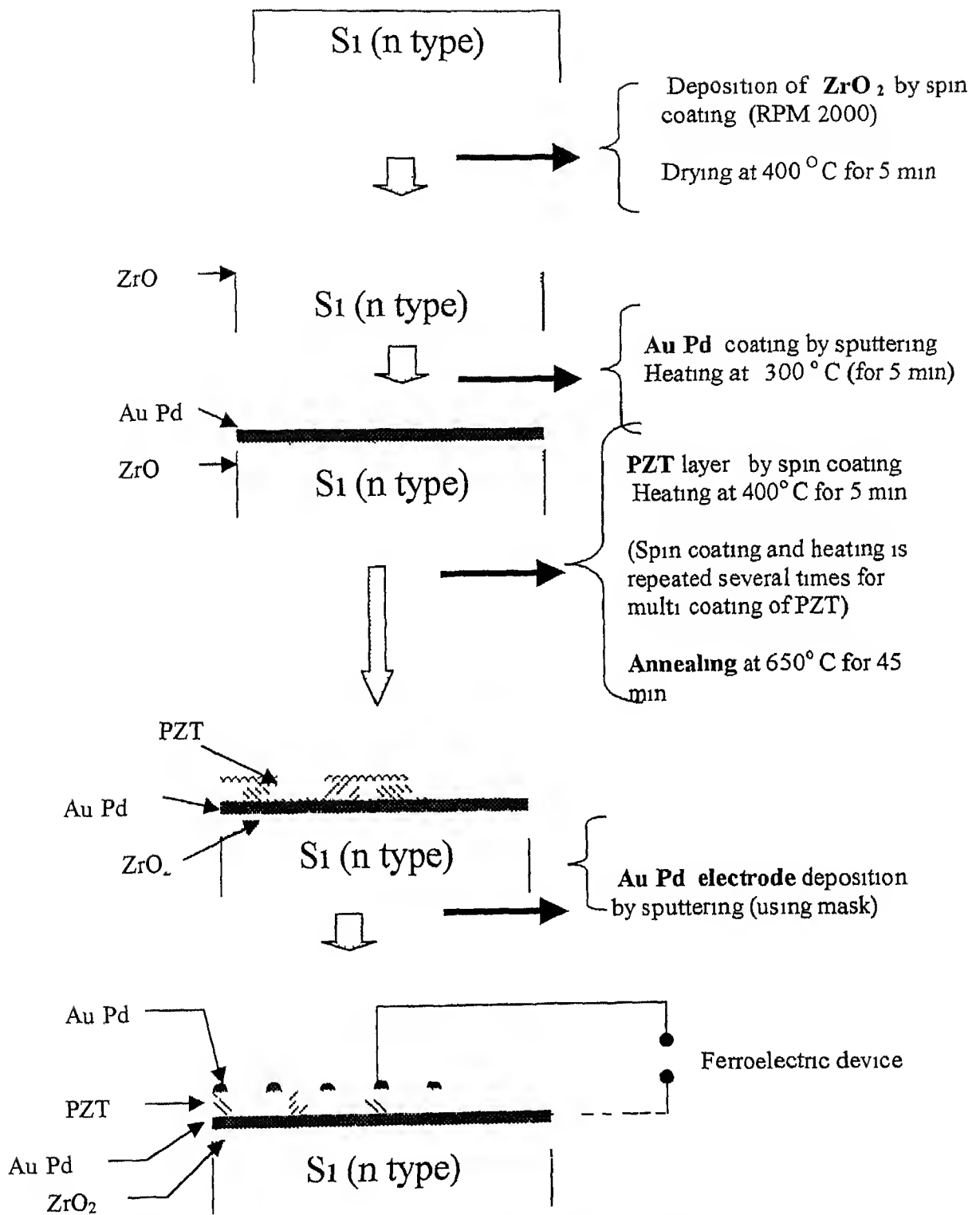


Fig 2 7 Au Pd/PZT/Au Pd/ZrO<sub>2</sub>/Si(100) sample preparation

## 2 3 CHARACTERIZATION

### 2 3 1 X-Ray diffraction

The X ray diffraction of thick films is carried out to determine the phases and lattice parameter of PZT X ray diffractometer (Rich Seifert Iso Debye flex 2002 Germany) has been used for X Ray diffraction of PZT thick films CuK $\alpha$  radiation ( $\lambda=1.5405 \text{ \AA}$ ) is used Following operating conditions have been used

Characteristic	Values
Accelerating voltage	30 kV
Accelerating current	20 mA
Scanning speed	3 <sup>o</sup> /min in 2 $\theta$
Chart speed	30 mm/min
Time count	10 sec
Count per min (CPM)	2k

The value of the inter planer spacing (d) is used to calculate the index of an X ray line using the Bragg relation

$$2d \sin \theta = n \lambda$$

where  $\theta$  = Bragg angle

n = order of diffraction

$\lambda$  = X ray wave length (1.54  $\text{\AA}$ )

For tetragonal system

$$\frac{1}{d^2} = \left( \frac{h^2 + K^2}{a^2} \right) + \left( \frac{l^2}{c^2} \right)$$

where h k and l are miller indices of the tetragonal system

## 2 3 2 Complex impedance analysis

### 2 3 2 1 Introduction

Sandwiched PZT thick layer between top and bottom (Au Pd) electrode acts as a ferroelectric capacitor with some dielectric values. The equivalent circuit for such arrangement can be expressed as a parallel combination of a resistor (R) and capacitor (C) for R C parallel combination. Net impedance  $Z(\omega)$  can be represented as follows:

$$\text{Net Impedance } Z(\omega) = \frac{R \left( \frac{1}{j\omega C} \right)}{R + \left( \frac{1}{j\omega C} \right)}$$

where

R= resistance

C=capacitance

$\omega$  = frequency

$$\text{Impedance } Z(\omega) = \frac{R}{Rj\omega C + 1}$$

$$= \frac{R}{1 + j\omega CR^2} \left( \frac{1 - j\omega CR}{1 - j\omega CR} \right)$$

multiplying numerator and denominator by  $(1 - j\omega CR)$

$$= \frac{R(1 - j\omega CR)}{1^2 - (j\omega CR)^2}$$



$$= \frac{R - R^2 j \omega C}{1 + \omega^2 C^2 R^2}$$

$$= \left( \frac{R}{1 + \omega^2 C^2 R^2} \right) + j \left( \frac{-R^2 \omega C}{1 + \omega^2 C^2 R^2} \right) \quad (1)$$

$$= Z \quad + j Z \quad (2)$$

On comparing equation (1) and equation (2)

$$Z = \left( \frac{R}{1 + \omega^2 C^2 R^2} \right) = Z \cos \theta \quad (3)$$

$$Z \left( \frac{-R^2 \omega C}{1 + \omega^2 C^2 R^2} \right) = Z \sin \theta \quad (4)$$

The above equation can be combined to give

$$\left( Z - \frac{R}{2} \right)^2 + (Z)^2 = \left( \frac{R}{2} \right)^2 \quad (5)$$

The equation (5) describes the equation of a circle of radius  $R/2$  with center at  $(R/2, 0)$

On plotting the graph between  $Z \cos \theta$  as X axis and  $Z \sin \theta$  as Y axis a semicircle will result having radius  $R/2$ . This is called Cole-Cole plot. The diameter of semicircle gives the value of resistance ( $R$ ). Similarly the admittance value  $Y(\omega)$  can be determined from impedance values

$$Y(\omega) = \frac{1}{Z(\omega)} \quad (6)$$

$$Y(\omega) = Y + j Y \quad (7)$$

where  $Y = 1/R = Y \cos \theta$

$Y = \omega C_p = Y \sin \theta$

$R$  = resistance

$C_p$  = measured capacitance

Dielectric constant and dielectric loss

$$\text{Dielectric constant } \varepsilon = \varepsilon' - j\varepsilon'' \quad \text{---(8)}$$

$$\begin{aligned} &= \frac{Y}{\omega C_o} - j \left( \frac{Y}{C_o \omega} \right) \\ &= \left( \frac{\omega C_p}{\omega C_o} \right) - j \left( \frac{1}{RC_o \omega} \right) \\ &= \left( \frac{C_p}{C_o} \right) - j \left( \frac{1}{RC_o \omega} \right) \quad \text{---(9)} \end{aligned}$$

Here  $C_o$  is the capacitance with no dielectric materials

On comparing equation (8) and equation (9)

$$\varepsilon' = \frac{C_p}{C_o} \quad \text{---(10)}$$

$$\varepsilon'' = \frac{1}{RC_o \omega} \quad \text{---(11)}$$

Dielectric loss (D) or loss tangent can be define as

$$\text{Loss tangent (D)} = \tan(\delta)$$

$$= \frac{\varepsilon''}{\varepsilon'}$$

$$= \left( \frac{1/RC_o \omega}{C_p/C_o} \right)$$

$$D = \frac{1}{R\omega C_p}$$

where  $R$  = resistance

$C_p$  = measured capacitance

## 2 3 2 2 Measurements

Impedance Analyzer 4192A LF (Hewlett Packard 5Hz 13MHz) was used for accurate measurement of impedance parameters of PZT ferroelectric thick films having different PVP (monomer)/Ti molar ratios. For measurement, the frequency range was chosen between 100Hz to 12MHz range. Oscillator level was kept constant at 0.25V.

On plotting Cole-Cole plot, more than one semicircles were obtained in some samples. Jie Lue et al. (33) have shown the Cole-Cole plot for yttrium stabilized zirconium ceramic. For  $Y_2O_3$ - $ZrO_2$ , three separate semicircles associated with grain interior, grain boundary and electrode interface are obtained. In  $Y_2O_3$ - $ZrO_2$  ceramic, the relatively small grain interior resistance  $R_g$  results in a small relaxation time which dominates at higher frequency range. The relaxation for the grain boundary conduction is 3 orders of magnitude higher than that for grains, hence a separate semicircle is observed in low frequency range for the grain boundaries. The relaxation time for electrode/ceramic interface is even higher and contributes only in the very low frequency range. The grain boundary resistance  $R_{gb}$  is related to grain size, segregation of impurities and presence of other grain boundary phase. For PZT thick films with different PVP/Ti ratio, Cole-Cole plots have been obtained at temperatures ranging from 75°C to 250°C. From the radius of the semicircles, the DC resistance of PZT ceramic film with different PVP/Ti ratio can be obtained.

Frequency dependence of dielectric properties can be expressed in terms of dielectric constant and complex impedance ( $Z^*$ )

$$\epsilon = \left( \frac{C_p}{C_o} \right) - j \left( \frac{1}{RC_o\omega} \right)$$

and loss tangent ( $D$ ) =  $\tan(\delta)$

$$D = \frac{1}{R\omega C_p}$$

For an ideal parallel RC circuit the conductivity is independent of frequency and the real and imaginary parts of the circuit impedance form a full semicircle when plotted between  $Z \cos \theta$  as X axis and  $Z \sin \theta$  as Y axis. But in actual practice depressed semicircle is obtained. Also in real materials the dielectric loss is not proportional to  $1/\omega$  but can be characterized by Jonscher's universal expression (34)

$$\varepsilon = \text{constant} \left( \frac{\omega}{\omega_p} \right)^{n_1-1} + \left( \frac{\omega}{\omega_p} \right)^{n_2-1}$$

where  $\omega_p$  = characteristic frequency which in dipolar dielectric is associated with the frequency of dielectric loss peak and  $n_1, n_2 = 0$  to 1

### 2.3.3 Dielectric constant

PZT used as a high dielectric constant material. Capacitance of PZT film can be directly measured from impedance analyzer. Film thickness of PZT deposited on Au/Pd/ZrO<sub>2</sub>/Si(100) can be determined using a profilometer ( $\alpha$  Step 100 Tencor Instruments). The average area of top electrode was determined by optical microscopy at 100 magnification. Average area of electrode was found to  $0.196 \times 10^{-6} \text{ m}^2$ . The complete specimen Au/Pd/PZT/Au/Pd/ZrO<sub>2</sub>/Si(100) acts as parallel plate capacitor where Au/Pd acts as top and bottom electrodes and PZT as dielectric material. The dielectric constant of PZT thin film was determined by using simple capacitor theory

$$C = \frac{\varepsilon_0 \varepsilon_{\text{pzt}} A}{d}$$

$C$  = capacitance of dielectric materials

(Directly measured from impedance analyzer)

$A$  = area of top electrode

$\epsilon_{PZT}$  = dielectric constant of PZT dielectric material

$d$  = thickness of PZT film

The capacitance and the dielectric loss of the device are read directly from the impedance analyzer. Measurements were carried out between 100 Hz to 1 MHz. However, the dielectric constant was found to become nearly constant after 100 KHz, and so the data only up to 100 KHz is presented for better resolution.

# Chapter 3

---

## 3 Result and discussion

PZT films from sols with different PVP/Ti ratio have been deposited on Au Pd/ZrO<sub>2</sub>/Si(100) n type substrates by spin coating. Sols with different PVP/Ti ratio were prepared. The volume of the as prepared sol in each case was maintained at 16 ml. This original sol with different PVP/Ti ratio has a concentration of 0.63M. From each sol 5ml of volume was taken and diluted by adding a 5 ml mixture of isopropyl alcohol and acetic acid (each 2.5 ml). The total volume of sol (10 ml) was stirred for 10 min. This produced a sol of concentration of 0.32 M. Films were deposited from this sol also. Unless otherwise mentioned, 10 coatings were made in each case. Baking between the coatings was done at 400°C for 5 min and the final annealing was done at 650°C for 45 min.

### 3.1 X-ray diffraction

A ZrO<sub>2</sub> film was first deposited on Si (100) -n type substrate by spin coating and heat treated at 400°C. ZrO<sub>2</sub> coating over Si substrate prevents the diffusion of Si and Pb through interface. X ray diffraction of ZrO<sub>2</sub> thin layer deposited over silicon after annealing at 650°C for 30 min is shown in fig (3.1). A cubic ZrO<sub>2</sub> phase is obtained.

During the actual sample preparation the  $\text{ZrO}_2$  film was annealed at  $400^\circ\text{C}$  followed by Au Pd bottom electrode deposition After the deposition of the PZT film the whole combination was annealed at  $650^\circ\text{C}$  The phases present in the PZT films have been determined by X ray diffraction Fig 3 2(a) and fig 3 2(b) show the X ray diffractograms for PZT with no PVP and with PVP respectively The data has been tabulated in table 3 1 Peaks positions match with pervoskite structure [32]

**Table3 1 X ray diffraction data for PZT (Perovskite Structure)**

<b>Diffraction angle (<math>2\theta</math>)</b>	<b>Relative Intensity (<math>I/I_0</math>)</b>	<b>Plane</b>	<b>d-(<math>\text{\AA}</math>)</b>
20 70	46 6	(100)	4 2901
30 01	100	(110)	2 977
38 81	51 11	(111)	2 349
43 59	43 59	(200)	2 0764
57 53	54 4	(211)	1 686

A  $\text{ZrO}_2$  film was first deposited on Si (100) -n type substrate by spin coating and heat treated at  $400^\circ\text{C}$   $\text{ZrO}_2$  coating over Si substrate of prevents the diffusion of Si and Pb through interface X ray diffraction of  $\text{ZrO}_2$  thin layer deposited over silicon after annealing at  $650^\circ\text{C}$  for 30 min is shown in fig (3 1) A cubic  $\text{ZrO}_2$  phase is obtained During the actual sample preparation the  $\text{ZrO}_2$  film was annealed at  $400^\circ\text{C}$  followed by Au Pd bottom electrode deposition After the deposition of the PZT film the whole combination was annealed at  $650^\circ\text{C}$

### 3.2 Effect of PVP/Ti ratio

Effect on thickness of PZT thin films with different PVP/Ti molar ratios in sol has been shown in figure 3.3. The film thickness decreases a little with the first addition of PVP but then increases and becomes nearly constant. The initial decrease may be within the experimental scatter but this needs to be verified. Two different sol concentrations (0.32M and 0.63M) of PZT with different PVP/Ti molar ratio have been used for film preparation. Large film thickness is obtained from more concentrated sol. A decrease in the film thickness at the highest PVP concentration in case of the more concentrated sol was not expected and needs to be verified.

Dielectric loss of PZT films prepared by using different sol concentrations (0.32M and 0.63M) with different  $\text{PVP}_{\text{monomer}}/\text{Ti}$  molar ratios are shown in fig (3.4) and fig (3.5). The dielectric loss decreases at high frequencies. At two frequencies (50kHz and 100kHz) the effect of PVP/Ti molar ratio on dielectric loss is shown in fig (3.6). It can be seen that there is no clear correlation. It should be noted that due to the preparation procedure the concentration of acetic acid is different in the two sols (0.32M and 0.63M). The dielectric loss is plotted against the PVP/acetic acid ratio in fig (3.7). There appears to be tendency for the dielectric loss to become very high at an intermediate concentration (PVP/ acetic acid = 0.05 to 0.1) of acetic acid. Acetic acid has a significant effect on the sol gel chemistry. It can act as a chelating agent and inhibits the condensation reactions. This aspect needs to be further investigated. Effect of thickness on dielectric loss is shown in figure (3.8). At high frequency range, dielectric loss is almost independent of thickness.



Dielectric constant of PZT thick films with different sol concentrations (0.32M and 0.63M) and PVP/Ti molar ratios are shown in fig (3.9) and fig (3.10). In all cases the dielectric constant decreases with increase in the frequency. Sharp increases in the dielectric constant occur in frequency range from 1 to 20 kHz (fig 3.9 and fig 3.10). Effect of PVP/Ti ratio on the dielectric constant at 5 kHz and 100kHz are shown in fig (3.11). The dielectric constant is higher in the films prepared using the 0.63M sol because of the generally larger thickness. A high value of the dielectric constant is obtained at PVP/Ti = 0.5 in the film from 0.63M sol. Dielectric constants attain constant values of ~65 and ~130 at PVP/Ti ≥ 1.0 for sol concentration of 0.32M and 0.63M respectively. These values are on the low side of the range of values reported for the PZT films. Much higher dielectric constant can be obtained by increasing the film thickness to 11 μm. This thickness was obtained by using 21 coatings.

### 3.3 Impedance spectroscopy

Impedance measurements on the sample were carried out at different frequencies in the temperature range from 75°C to 250°C. The top electrode was made of Au/Pd with diameter of 0.5 mm (area =  $0.196 \times 10^{-6} \text{ m}^2$ ). The impedance data were plotted as Cole-Cole plots ( $Z \cos \theta$  vs  $Z \sin \theta$ ). As discussed in chapter 2, such a plot yields arcs of circle. In the most general case, three arcs corresponding to bulk (high frequency), grain boundary and electrode interface (low frequency) are obtained. The diameter of a half circle gives the corresponding resistance due to grains, grain boundary and the interface. The dc conductivity can be calculated by using the equation

$$\sigma_{dc} = \frac{1}{R} \left( \frac{l}{A} \right)$$

क प्रोग्राम  
आ. प्रो. र. र.  
अवधि-क्र. 133647

where  $R$  is the resistance as above and  $l$  and  $A$  are the film thickness and electrode area respectively. For the case of grain boundary conductivity, a knowledge of the grain size and grain boundary thickness is required. The grain boundary conductivity is given by

$$\sigma_{gb} = \frac{1}{R_{gb}} \frac{l}{A} \left( \frac{\delta_{gb}}{d_{gb}} \right)$$

where  $\delta_{gb}$  is the width of grain boundary and  $d_{gb}$  is the grain size. To carry out an order of magnitude estimate, we have taken  $\delta_{gb}$  to be 1.0 nm and  $d_{gb}$  as 0.1  $\mu\text{m}$  giving  $\delta_{gb}/d_g = 10^{-2}$ . Fig (3.13) to fig (3.18) show the Cole-Cole plots for samples at different temperatures. In most of the cases, the bulk and grain boundary semicircles are clearly obtained. The values of the corresponding dc conductivity calculated as above are given in table (3.3). The data are also plotted as  $\ln \sigma$  vs  $1/T$  and the activation energies are obtained from the slopes of the plots. The data for activation energy are listed in table (3.4). It is seen that the activation energy for grain conduction is 10.12 kJ/mole for most of the samples except for the sample with PVP/Ti ratios of 0.2 and 2.0 for which activation energies of 28.8 and 4.3 kJ/mole respectively are obtained. The activation energy for the grain boundary conduction tends to have values, which vary between 3 to 25 kJ/mole.

The above data is tentative and needs to be confirmed by several measurements. Physical origins of conduction in PZT thin film have been suggested to be based on model such as Schottky emission, Pool-Frenkel emission, space charge limited conduction, ionic conduction etc. The dc conductivity measurements are usually carried out by measuring the leakage currents at different films. There are not many reports using impedance

measurements. It is demonstrated here that the impedance data are sensitive to the additive concentration and film thickness and thereby on the film microstructure. Hence it would be worthwhile to explore the technique further for understanding the conduction process in PZT films. The Cole-Cole plots for thick film are shown in fig (3.21-3.23). For the  $4.0\text{ }\mu\text{m}$  thick film, an arc is obtained but diameter of semicircle is large by nearly a factor of 10. For the  $4.6\text{ }\mu\text{m}$  thick sample, different behaviour showing parts of two semicircles are obtained.

**Table 3.3 DC conductivity of bulk and grain boundary for PZT with different PVP/Ti molar ratio**

S No	Sample details	T (°C)	DC conductivity ( $\sigma_{bulk}$ ) $\Omega^{-1}m^{-1}(10^3)$	DC conductivity ( $\sigma_{grain boundary}$ ) $\Omega^{-1}m^{-1}(10^5)$
1	PZT (no PVP)	74	0.22	0.068
	Sol Conc=0.32M	134	0.95	0.329
	Thickness=1.0 $\mu m$	245	1.53	0.97
2	PZT (PVP/Ti=0.2)	83	0.0047	—
	Sol Conc=0.32M	153	0.020	0.53
	Thickness=0.7 $\mu m$	246	0.110	—
3	PZT (PVP/Ti=0.5)	89	0.0179	0.034
	Sol Conc=0.32M	144	0.057	0.088
	Thickness=2.2 $\mu m$	256	0.069	0.106
4	PZT (PVP/Ti=1.0)	82	0.400	0.290
	Sol Conc=0.32M	168	0.587	0.285
	Thickness=1.8 $\mu m$	248	0.680	0.440
5	PZT (PVP/Ti=1.5)	93	0.170	0.240
	Sol Conc=0.32M	166	0.326	0.533
	Thickness=2.0 $\mu m$	245	0.480	0.42
6	PZT (PVP/Ti=2.0)	80	1.24	—
	Sol Conc=0.32M	135	1.46	
	Thickness=1.8 $\mu m$	245	2.10	

**Table3 4 Activation energy for PZT with different PVP/Ti molar ratio**

S No	Sample details	Activation Energy ( $E_a$ ) <sub>bulk</sub> (KJ/mole)	Activation Energy ( $E_a$ ) <sub>grain boundary</sub> (KJ/mole)
1	PZT (no PVP) Sol Conc=0.32M Thickness=1.0	12.72	24.7
2	PZT (PVP/Ti=0.2) Sol Conc=0.32M Thickness=0.7 $\mu m$	28.8	—
3	PZT (PVP/Ti=0.5) Sol Conc=0.32M Thickness=2.2 $\mu m$	10.7	10.4
4	PZT (PVP/Ti=1.0) Sol Conc=0.32M Thickness=1.8 $\mu m$	10.6	3.2
5	PZT (PVP/Ti=1.5) Sol Conc=0.32M Thickness=2.0 $\mu m$	10.1	6.9
6	PZT (PVP/Ti=2.0) Sol Conc=0.32M Thickness=1.8 $\mu m$	4.32	—

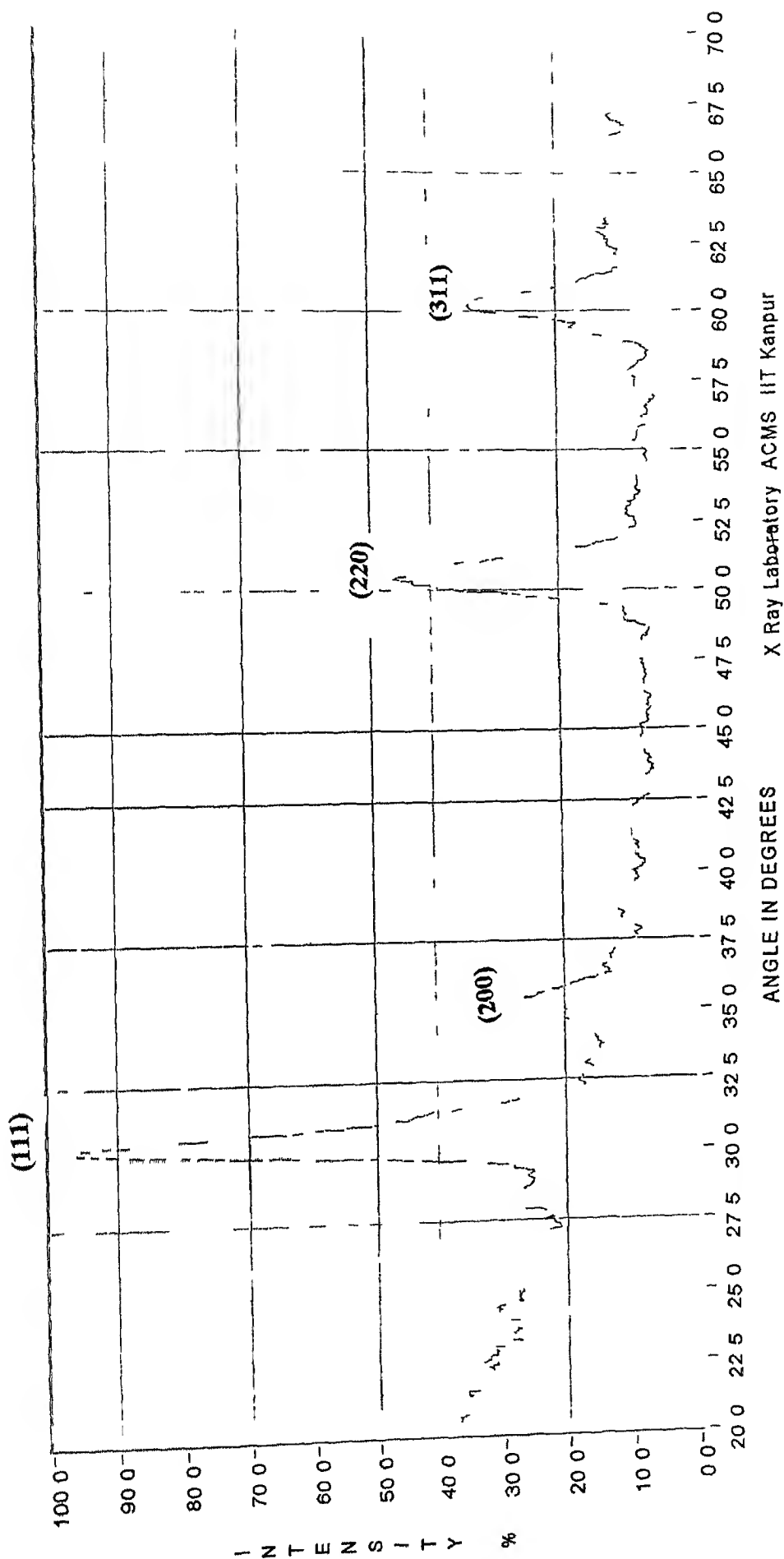


Fig3 1 X-ray diffractogram of  $ZrO_2$  films deposited on Si(100)-n type substrate (Annealing temperature is  $650^\circ C$ )

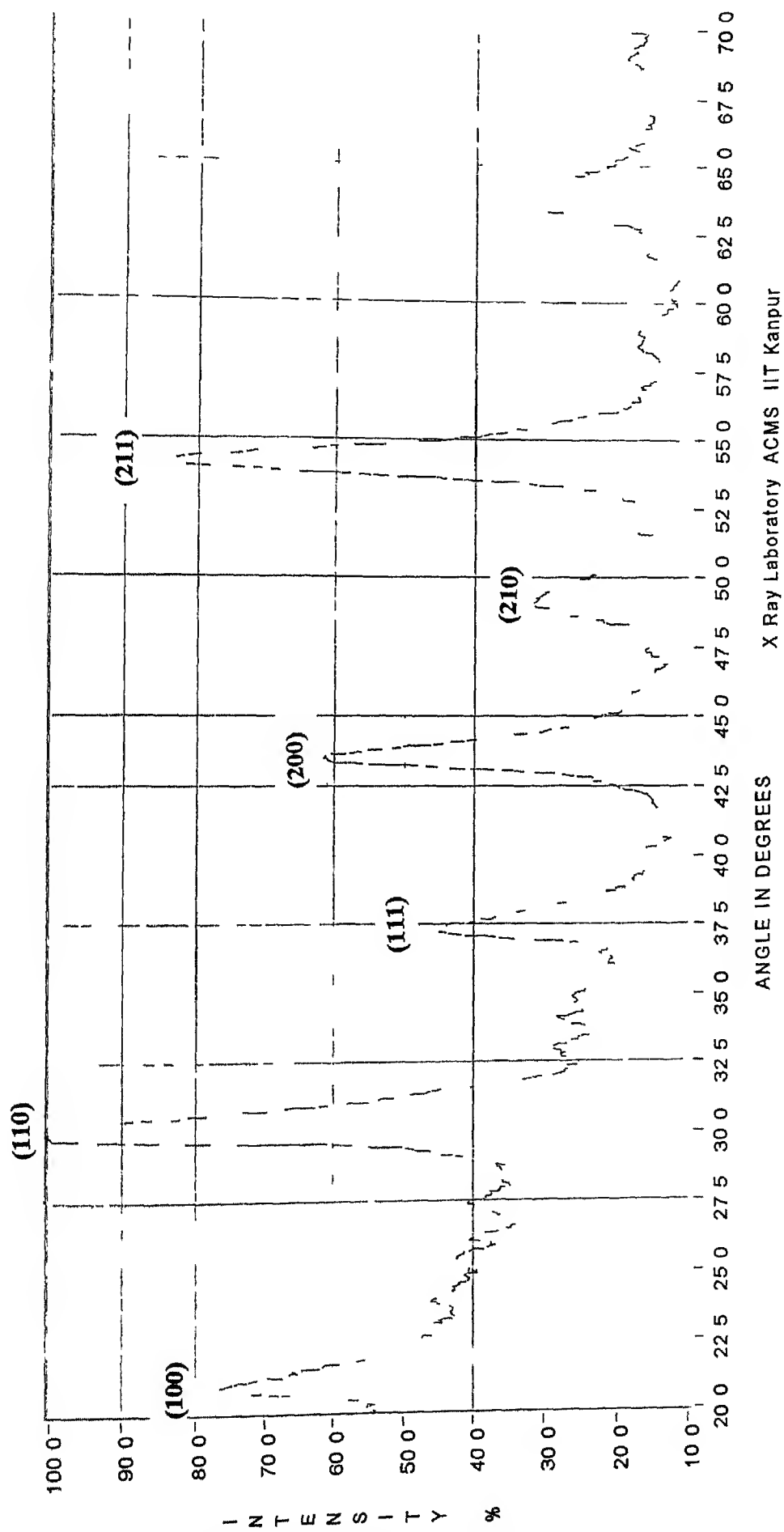


Fig 3 2(a) X-ray diffractogram of PZT films deposited on Au-Pd/ZrO<sub>2</sub>/Si(100) n type substrate (Annealing temperature is 650°C)

X Ray Laboratory ACMS IIT Kanpur

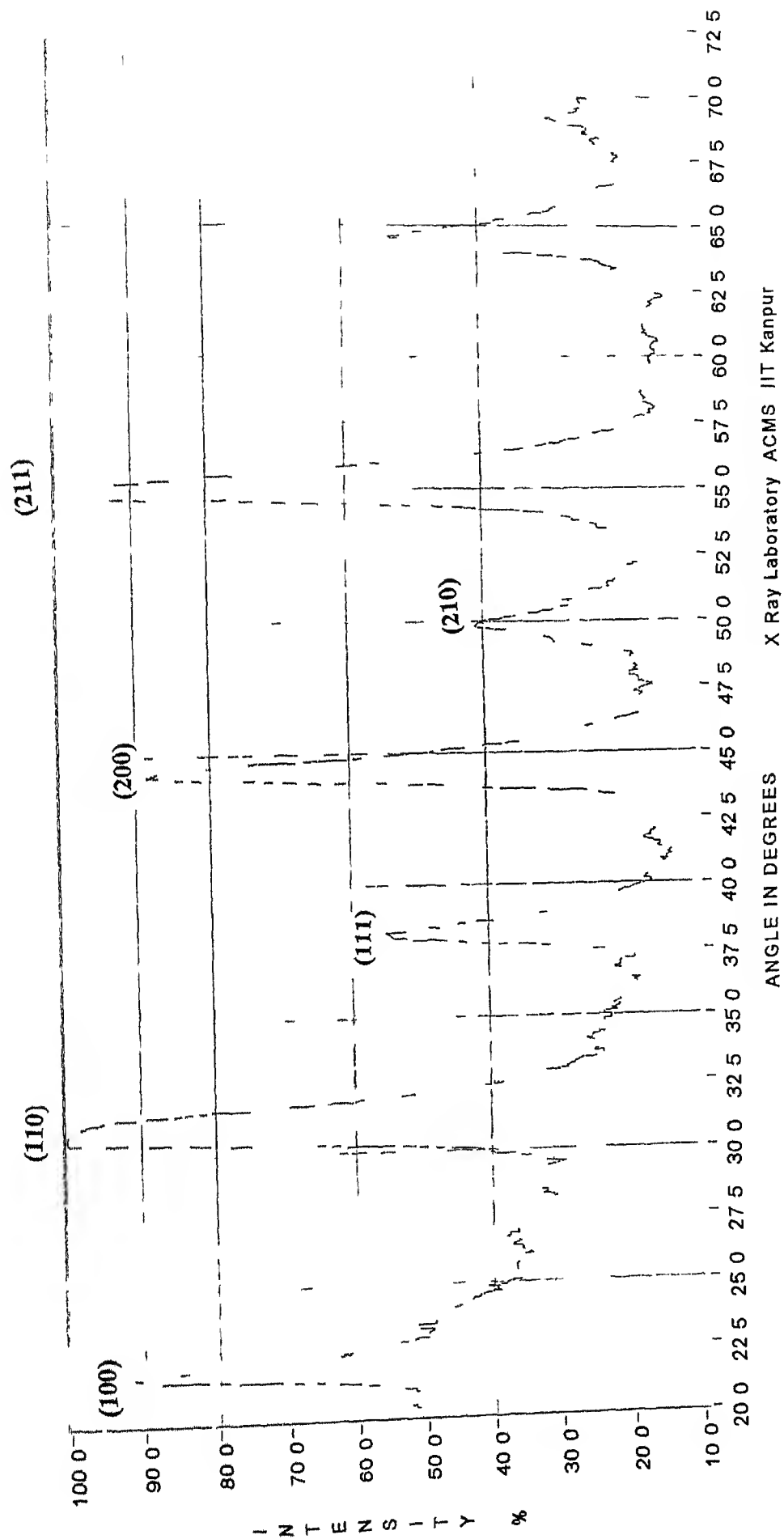


Fig3 2 (b) X ray diffractogram of PZT thin films with PVP(PVP/T<sub>1</sub>=1.0) deposited on Au Pd/ZrO<sub>2</sub>/Si(100)-n type substrate (Annealing temperature is 650°C)



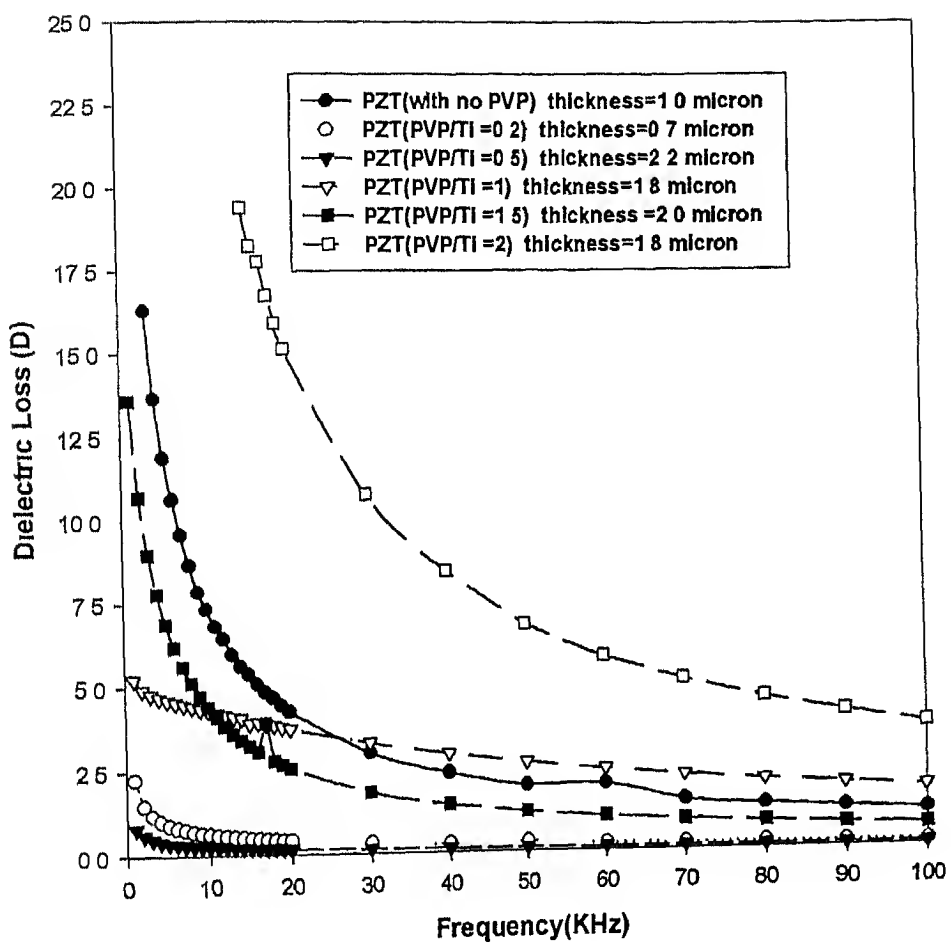


Fig 3.4 Frequency vs Dielectric Loss for PZT with Different PVP/Ti ratio (Sol Concentration is 0.32M)

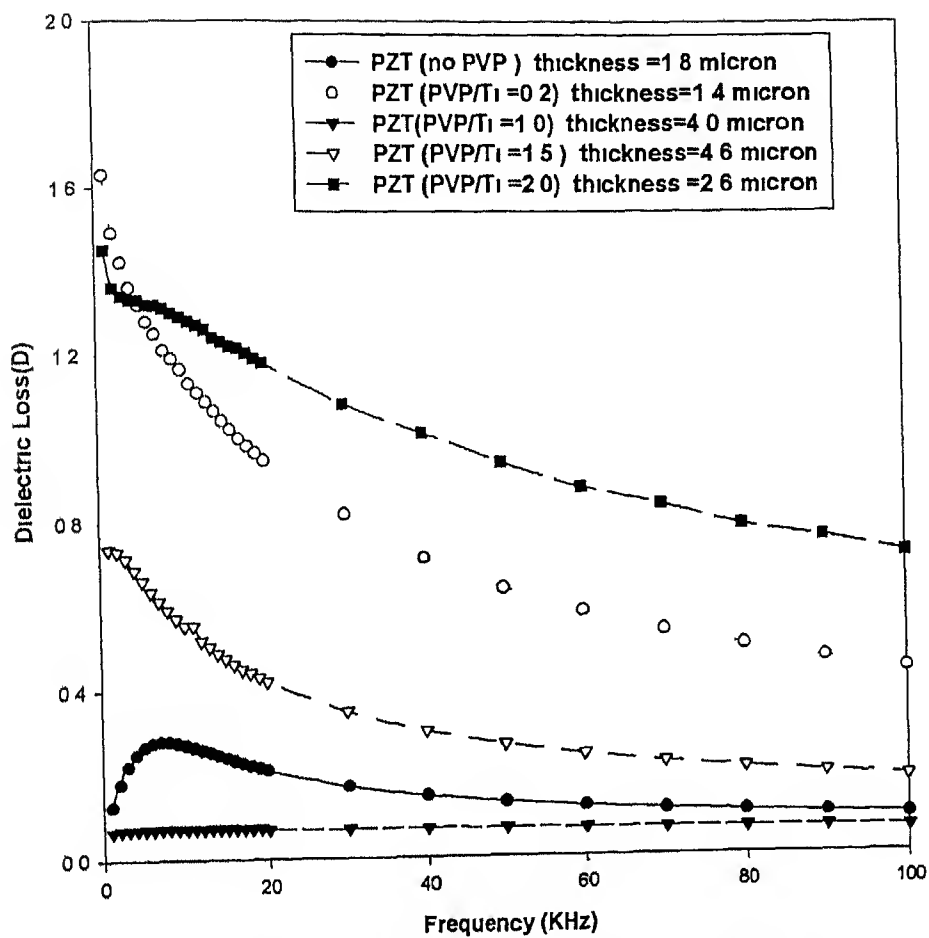


Fig 3.6 Frequency vs Dielectric Loss for PZT with different PVP/Ti molar ratio  
(Concentration of the sol is 0.63M. The loss was too high for PVP/Ti=0.5 to record)

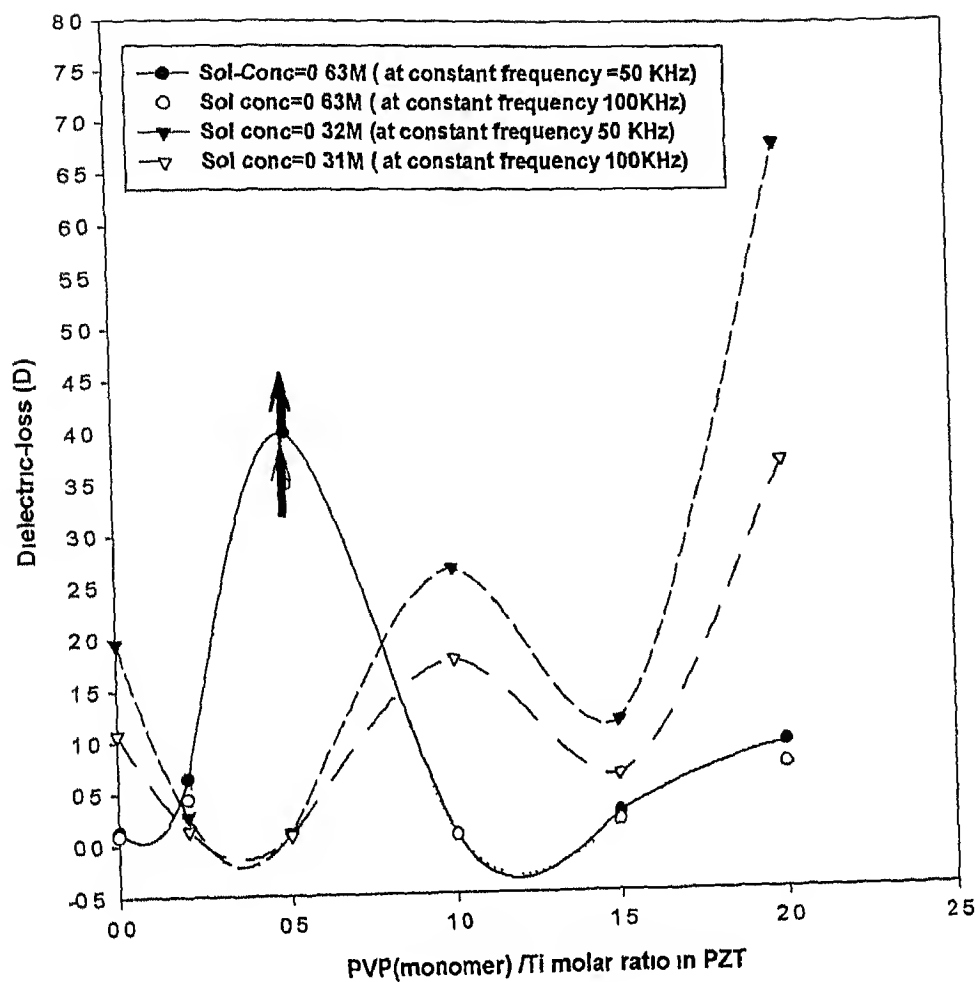


Fig 3.6 Effect of Sol concentration and PVP/Ti ratio on Dielectric loss

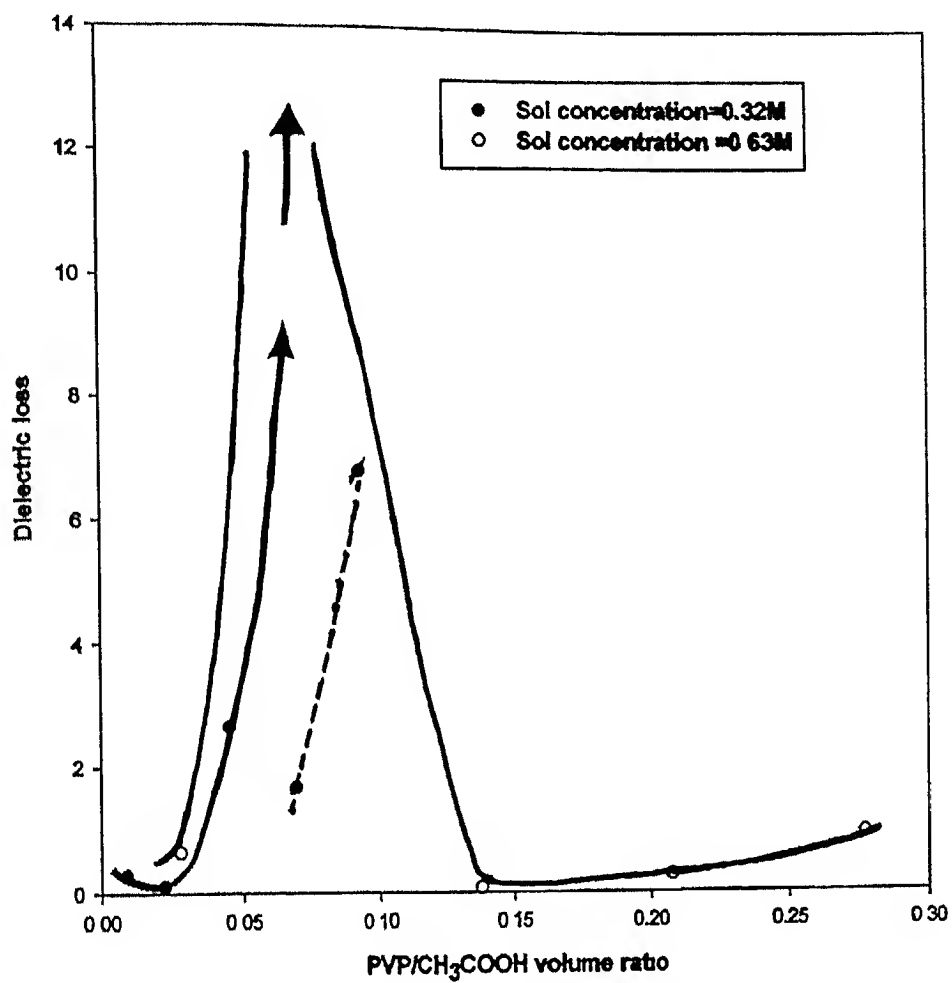
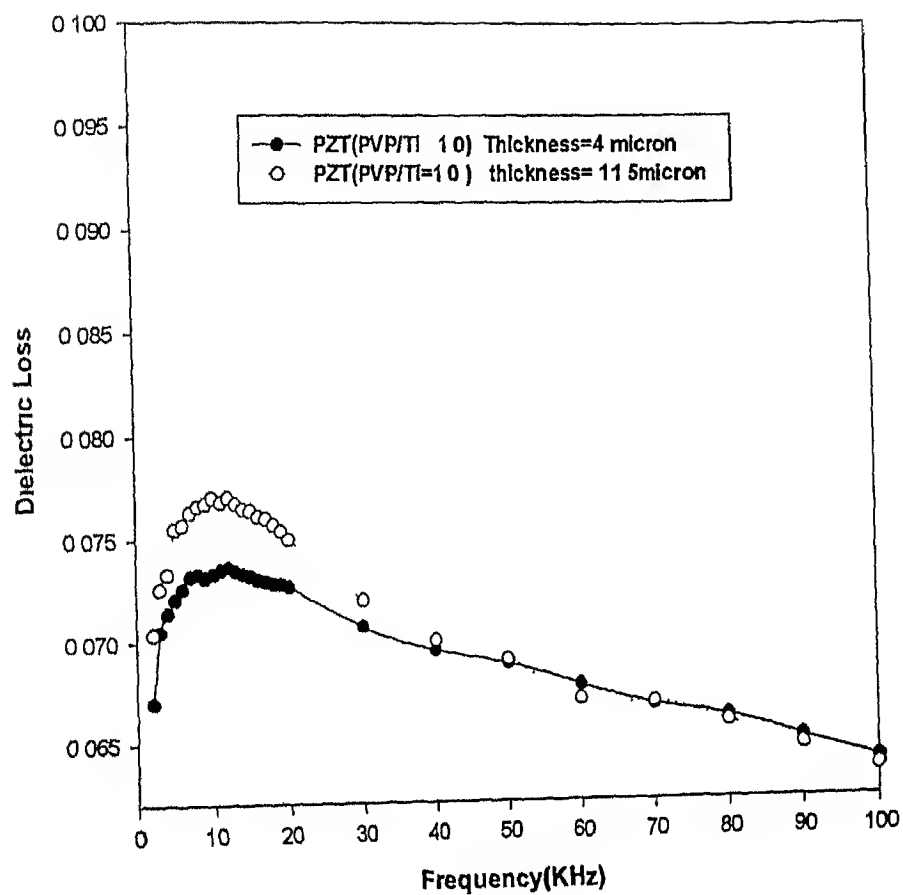


Fig 3 7 Effect of PVP/CH<sub>3</sub>COOH volume ratio on dielectric loss



**Fig 3 8 Effect of thickness on Dielectric Loss of PZT(PVP/Ti=1.0)  
( Sol concentration 0.63M)**

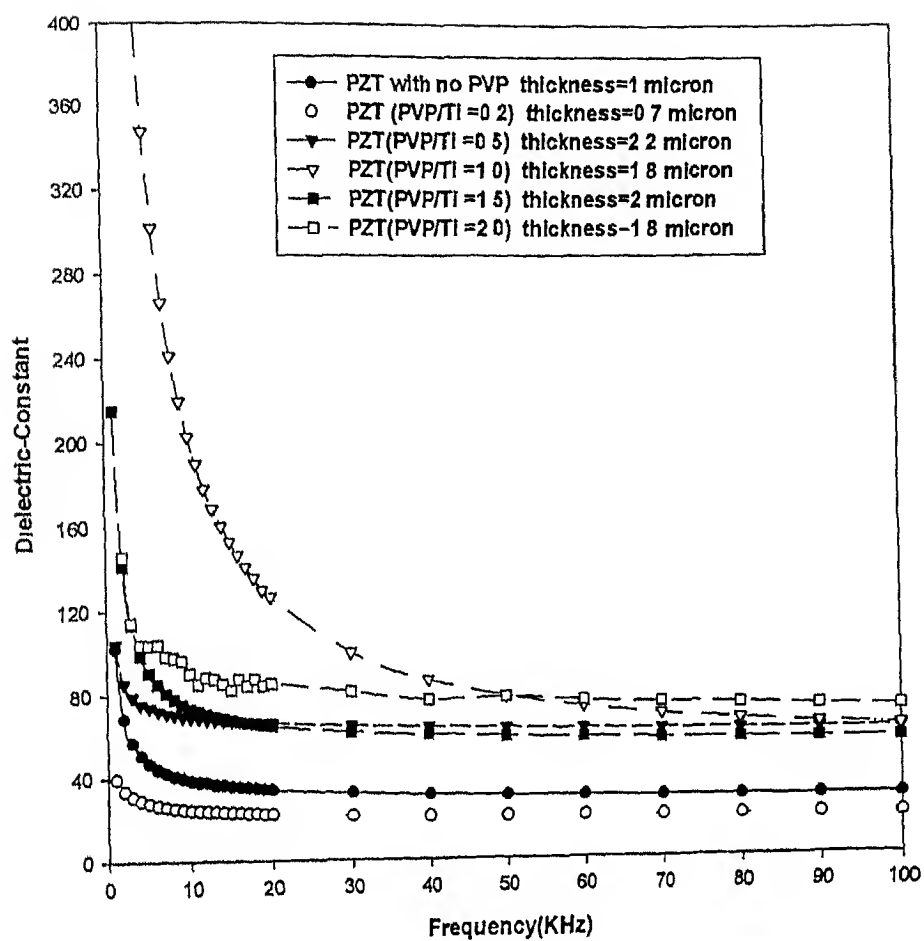


Fig 3.9 Frequency vs Dielectric Constant for PZT with different PVP/Ti ratio  
(Sol concentration 0.32M)

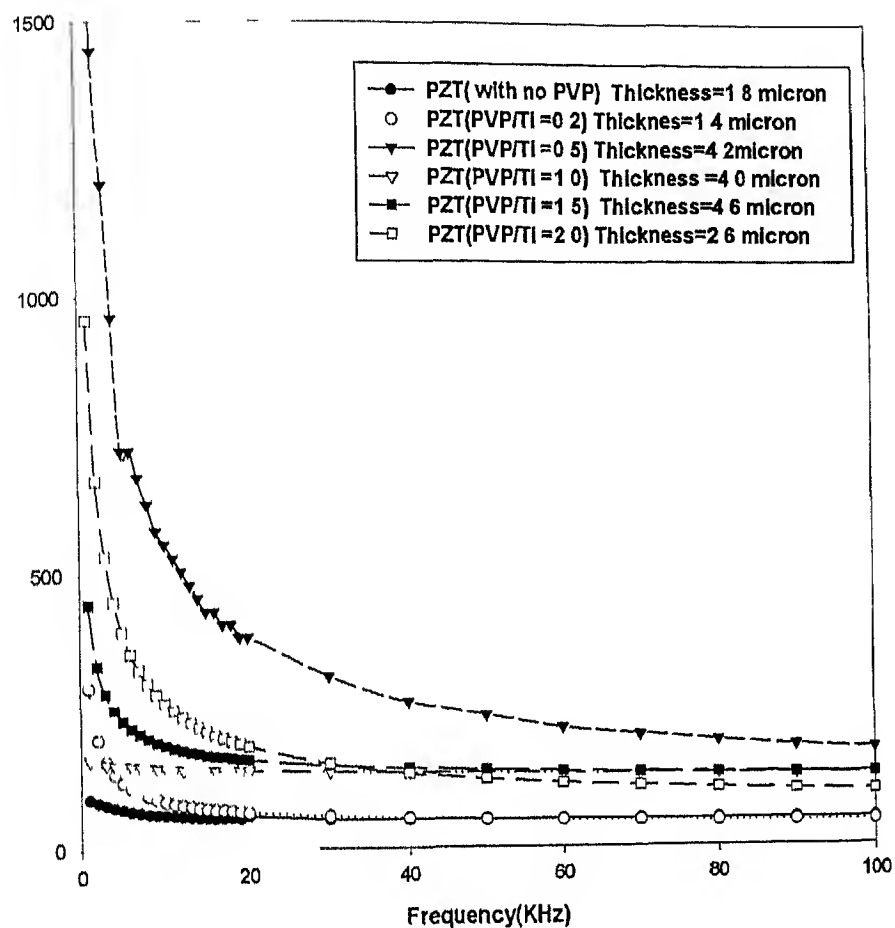


Fig 3 10 Frequency vs Dielectric Constant for PZT with different PVP/Ti ratio  
( Sol Concentration =0.63 M)

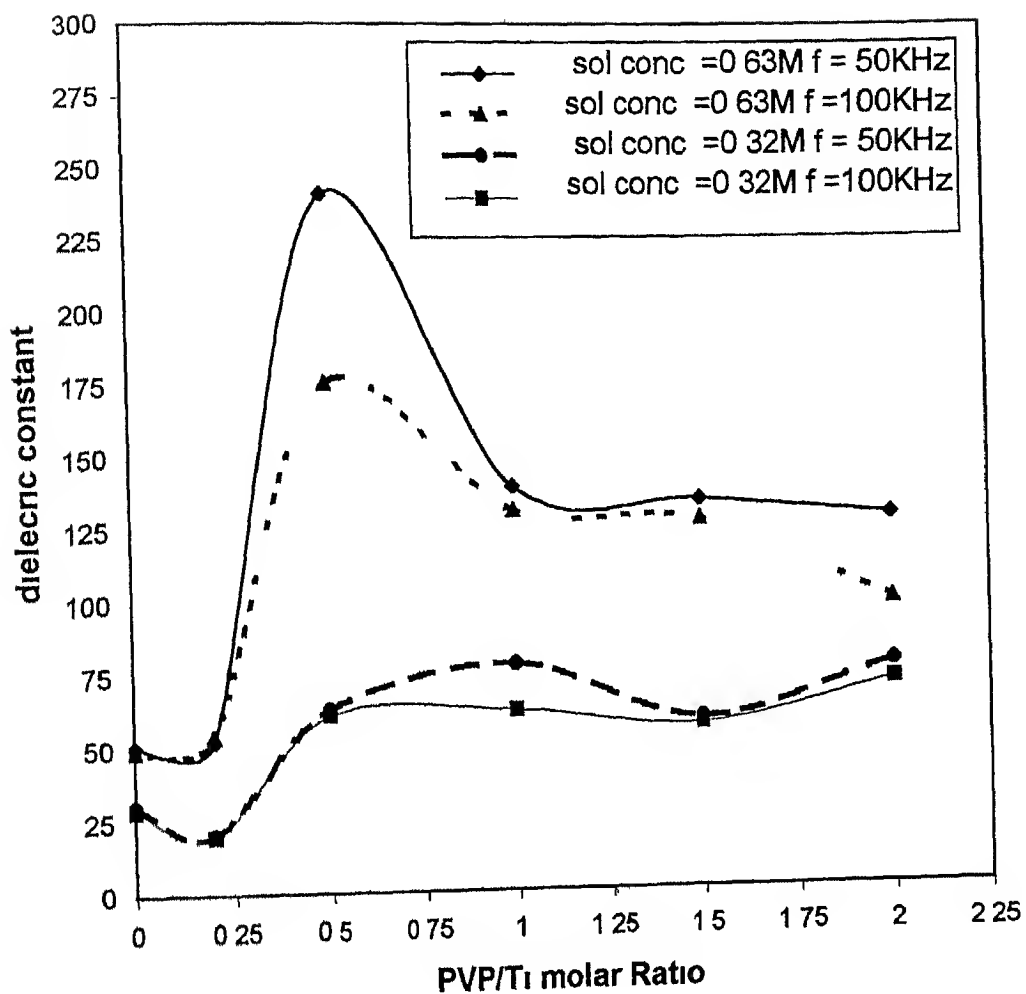
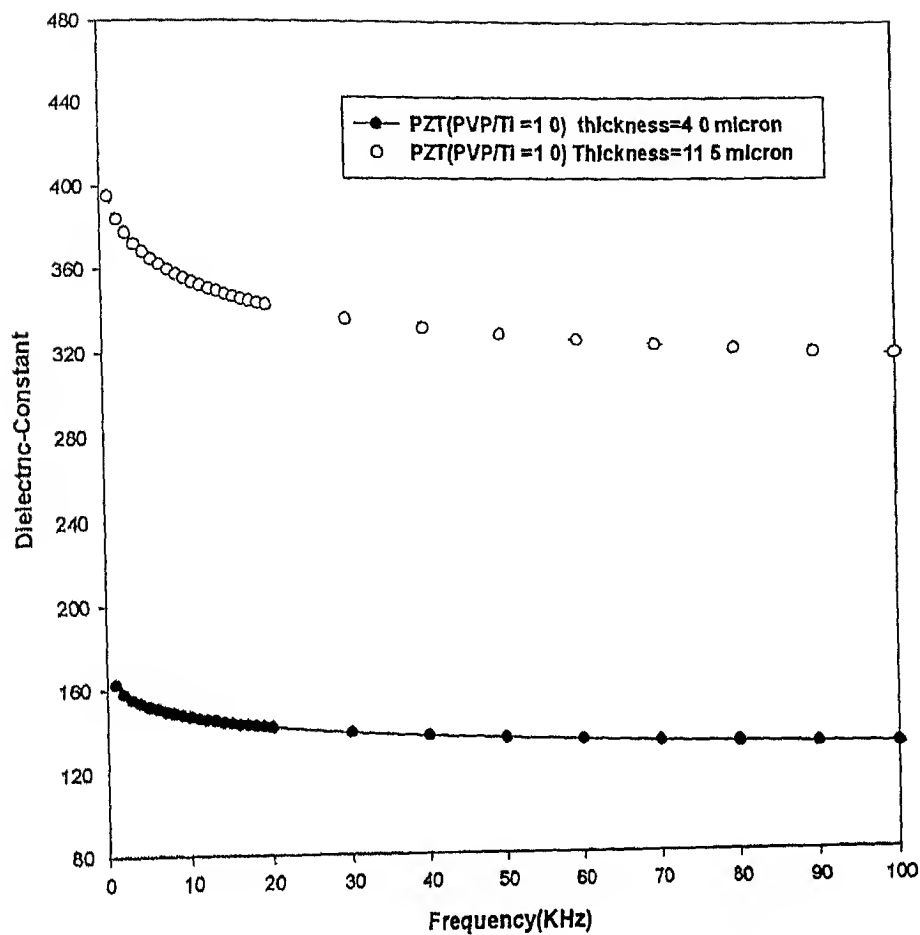
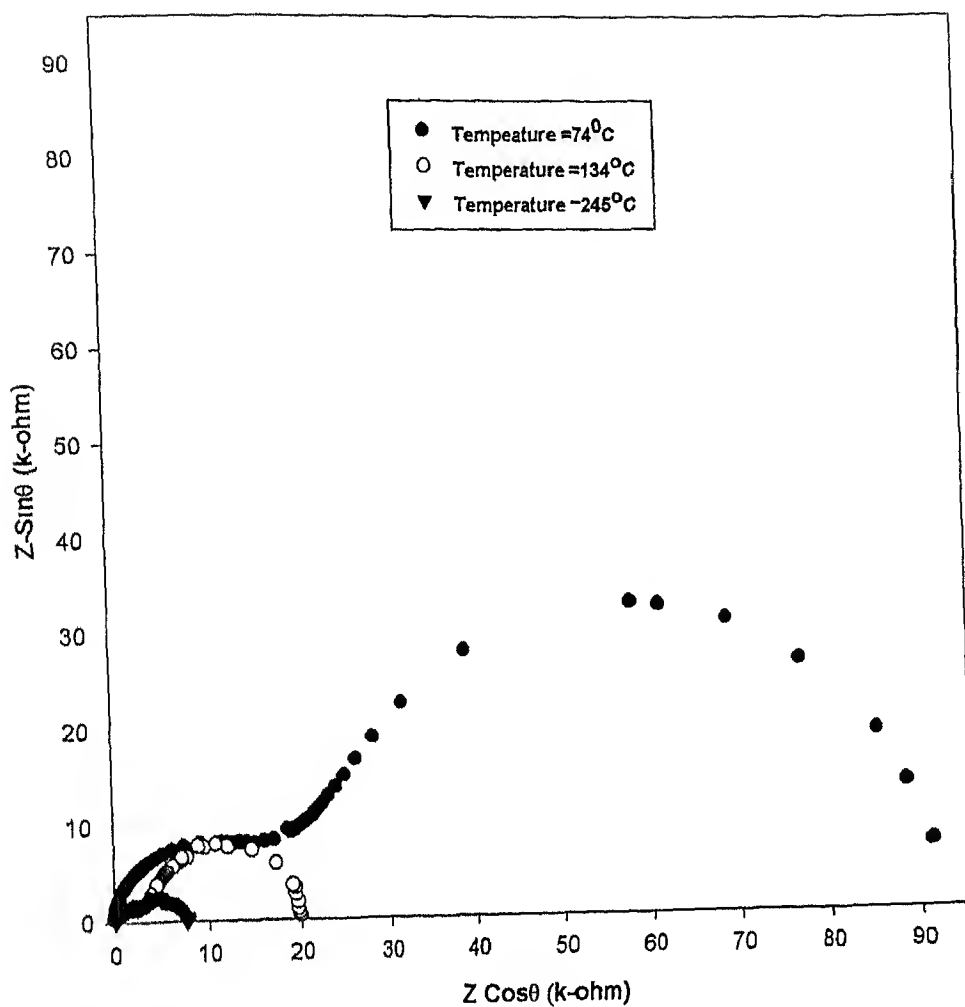


Fig 3 11 PVP/Ti Ratio vs Dielectric constant





**Fig 3 12 Effect of Thickness on Dielectric Constant**  
(Sol concentration of PZT(PVP/Ti=1.0) is 0.63M)



**Fig 3 13 Cole Cole plots for PZT (no PVP) at different temperatures  
(Sol concentration=0.32M)**

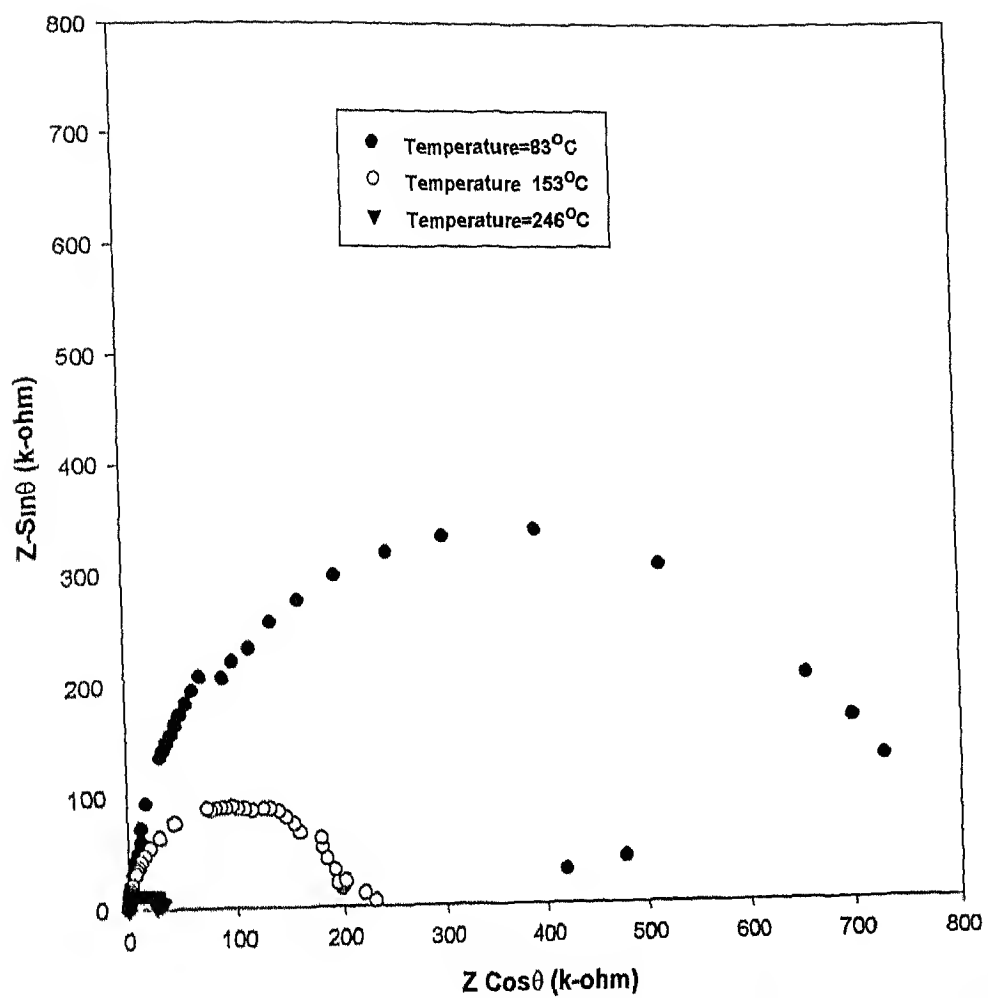


Fig 3 14 Cole Cole plots for PZT (PVP/Ti=0.2) at different temperatures (Sol concentration=0.32M)

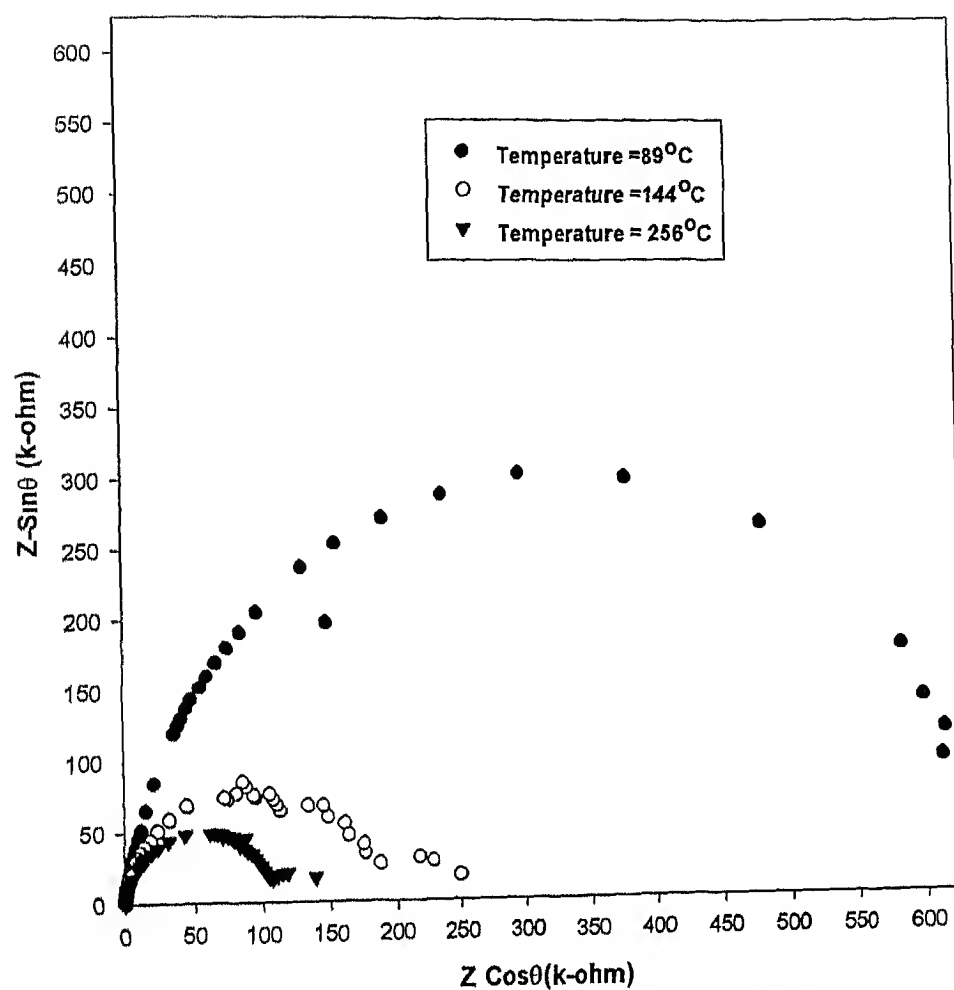


Fig 3 15 Cole Cole plots for PZT (PVP/Ti=0.5) at different temperatures  
(Sol concentration=0.32M)

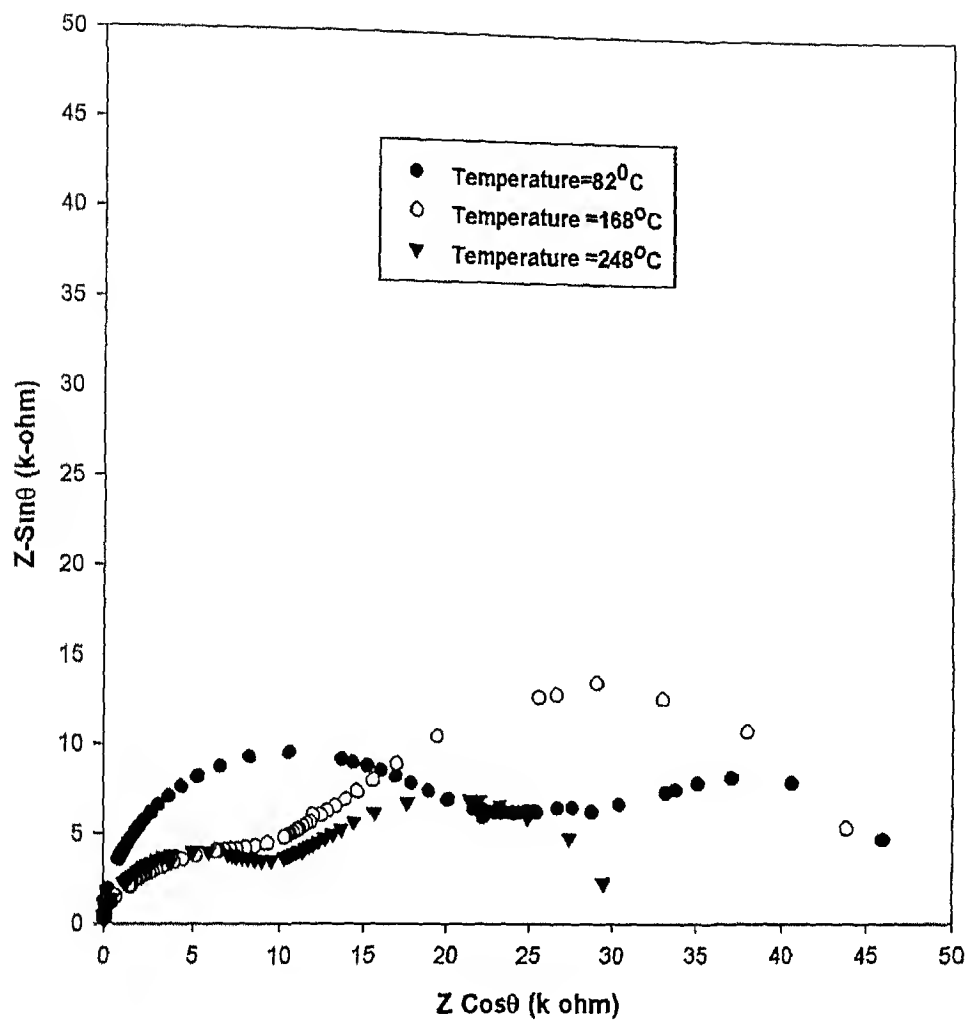


Fig 3 16 Cole Cole plots for PZT (PVP/Ti=1.0) at different temperatures (Sol concentration=0.32M)

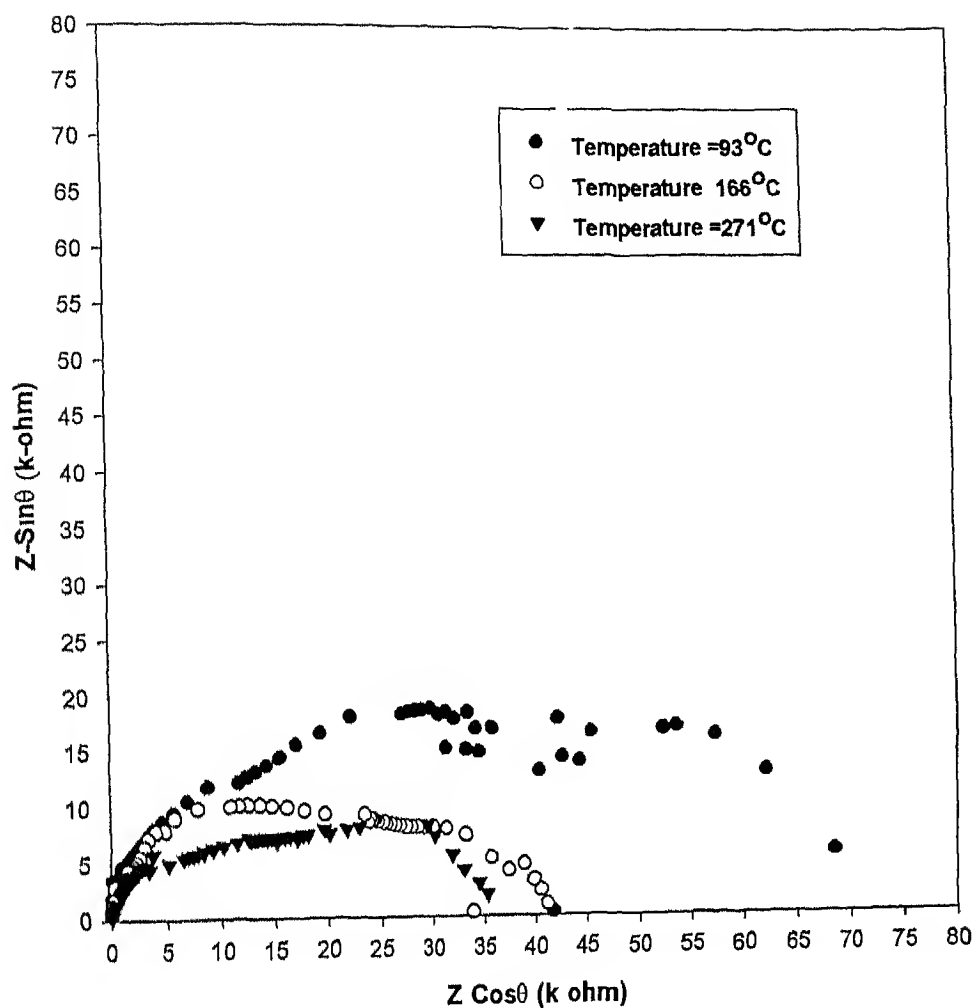
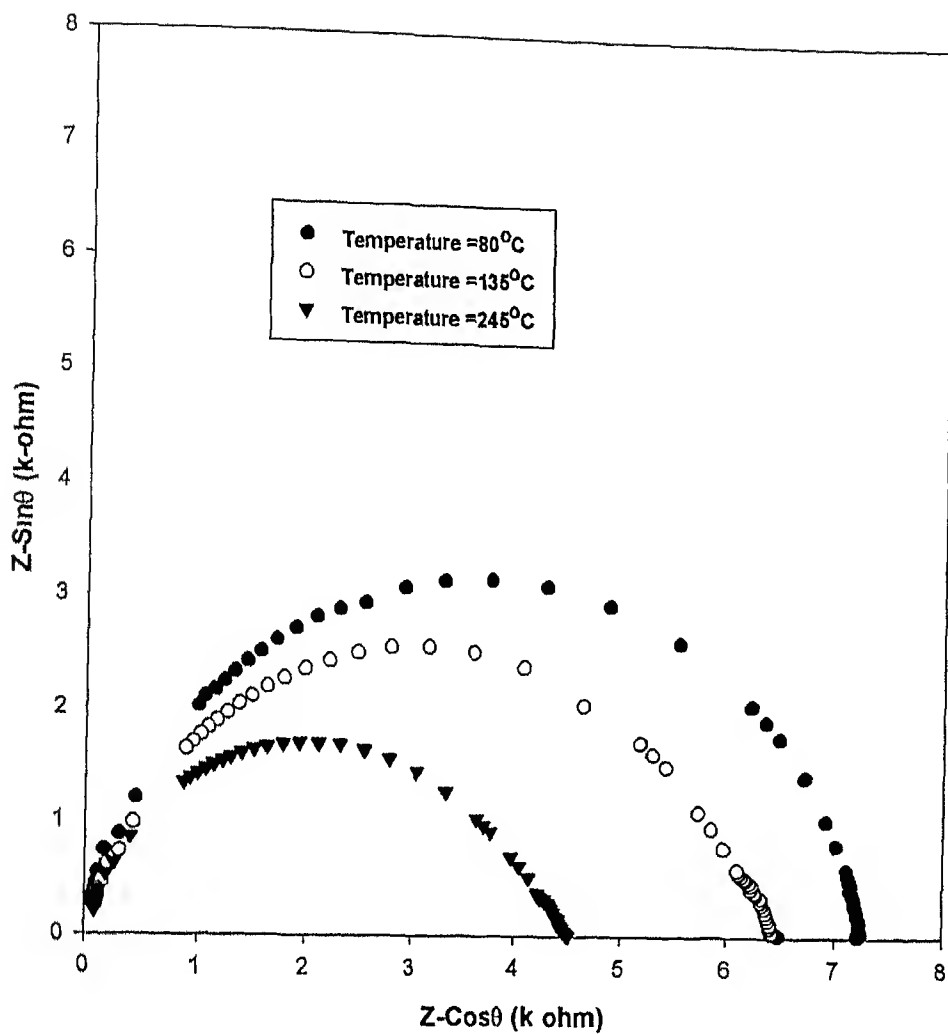
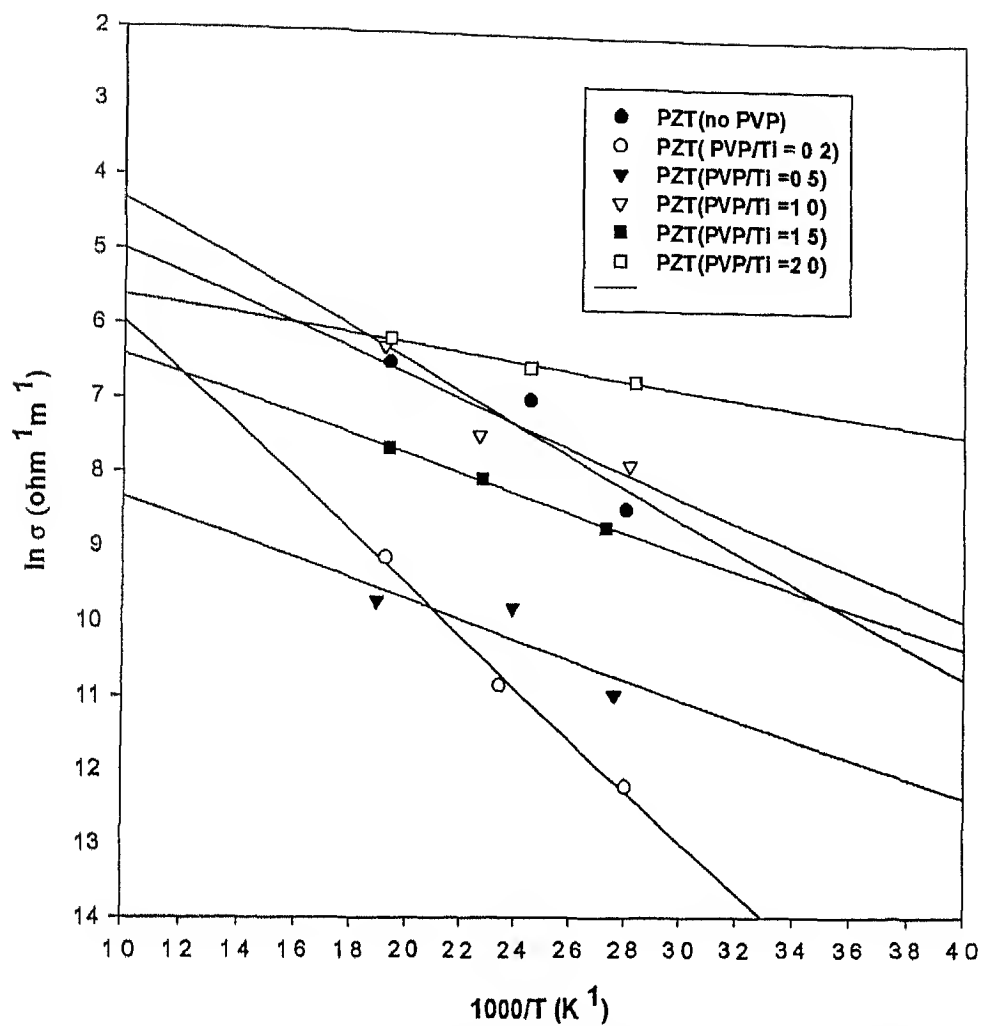


Fig 3 17 Cole Cole plots for PZT (PVP/Ti=1.5) at different temperatures  
(Sol concentration=0.32M)



**Fig 3 18** Cole Cole plots for PZT (PVP/Ti=2.0) at different temperatures  
(Sol concentration=0.32M)



**Fig3 19 DC Conductivity associated with grain interior of PZT with PVP present in sol in different PVP/Ti molar ratio (Sol concentration 0.32M)**



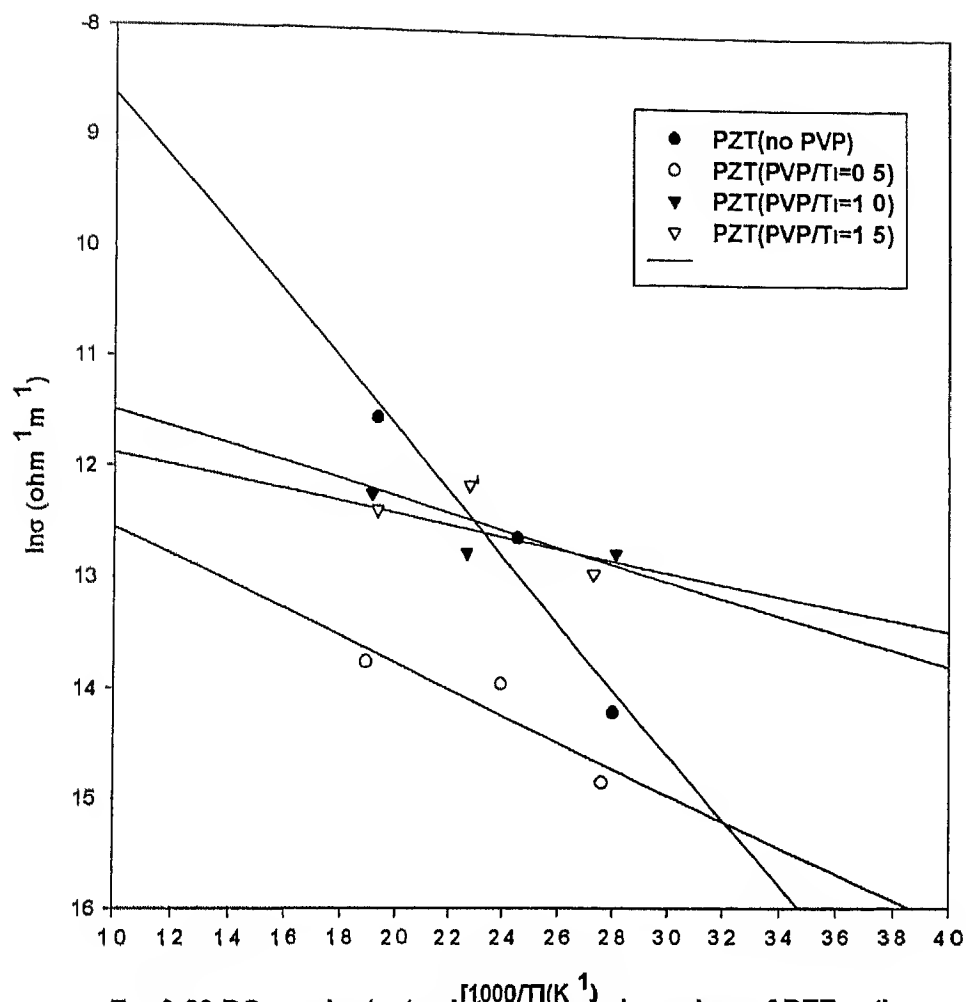


Fig 3 20 DC conductivity plots for grain boundary of PZT with PVP, present on sol in different PVP/Ti molar ratio (Sol concentration 0.32M)

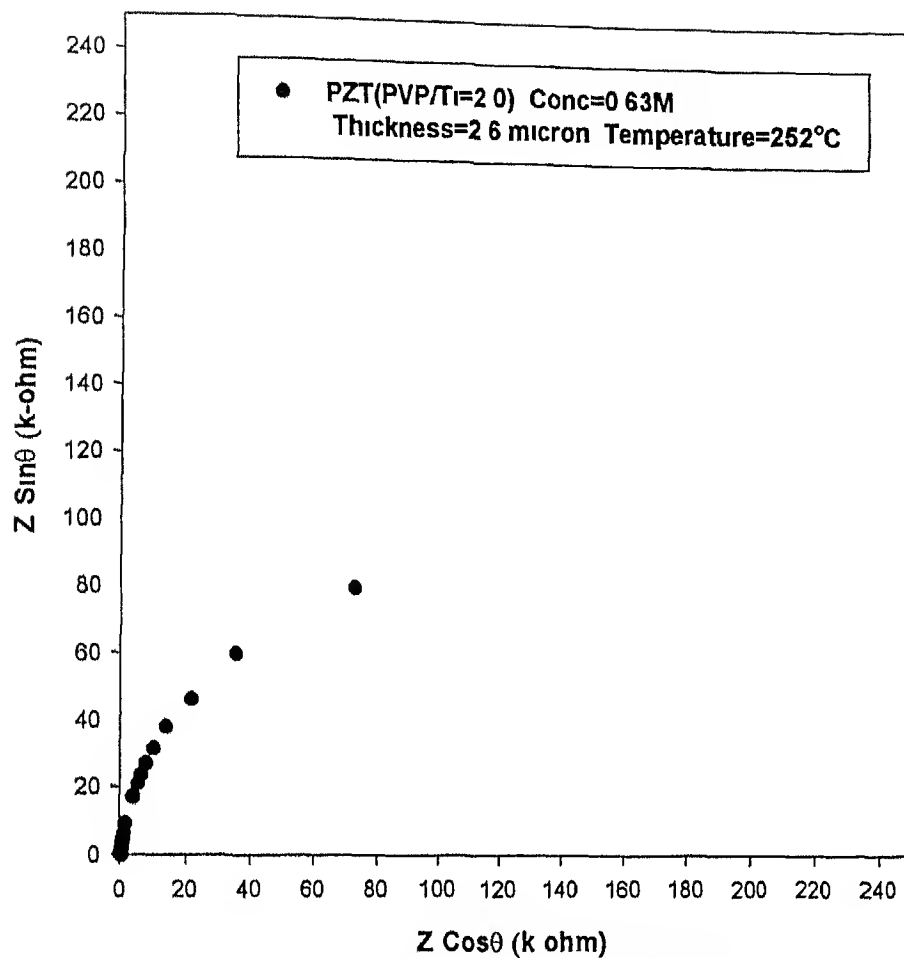
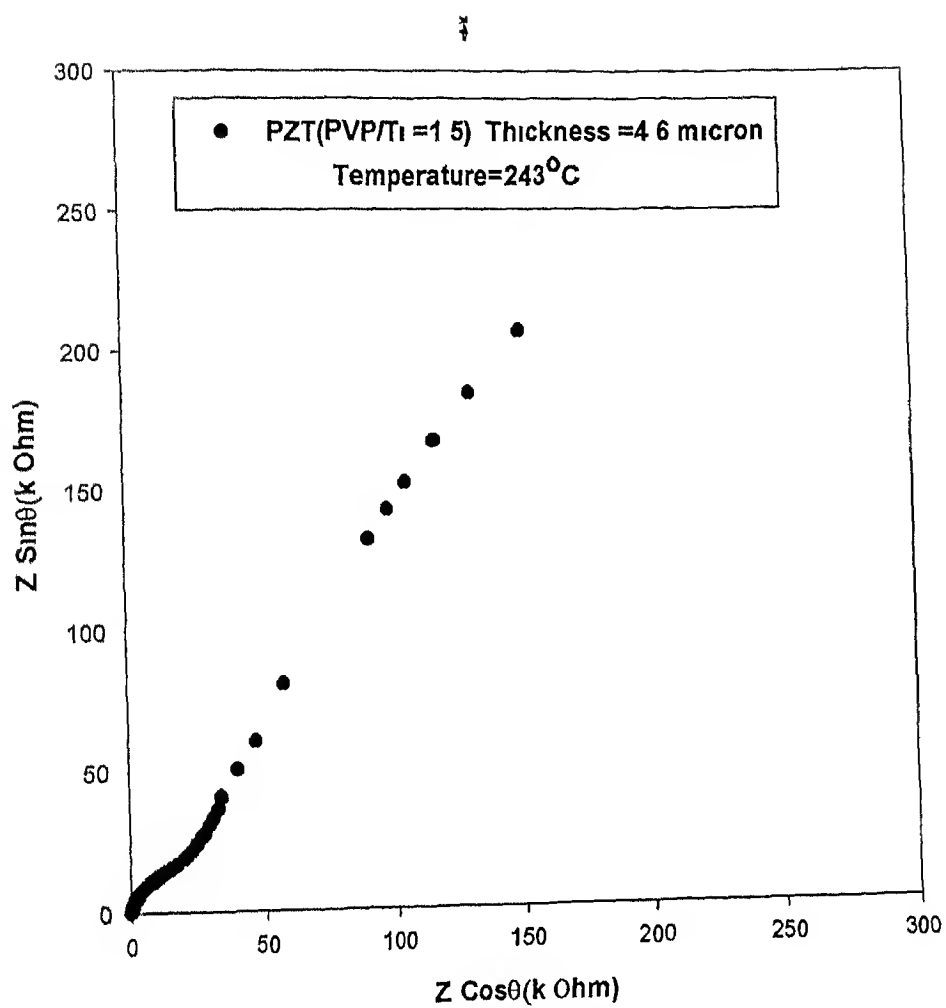


Fig 3.21 Cole Cole plot for PZT(PVP/Ti=2.0)  
(Sol Concentration=0.63M)



**Fig3.22** Cole Cole plot for PZT(PVP/Ti=1.5)  
(Sol concentration =0.63M)

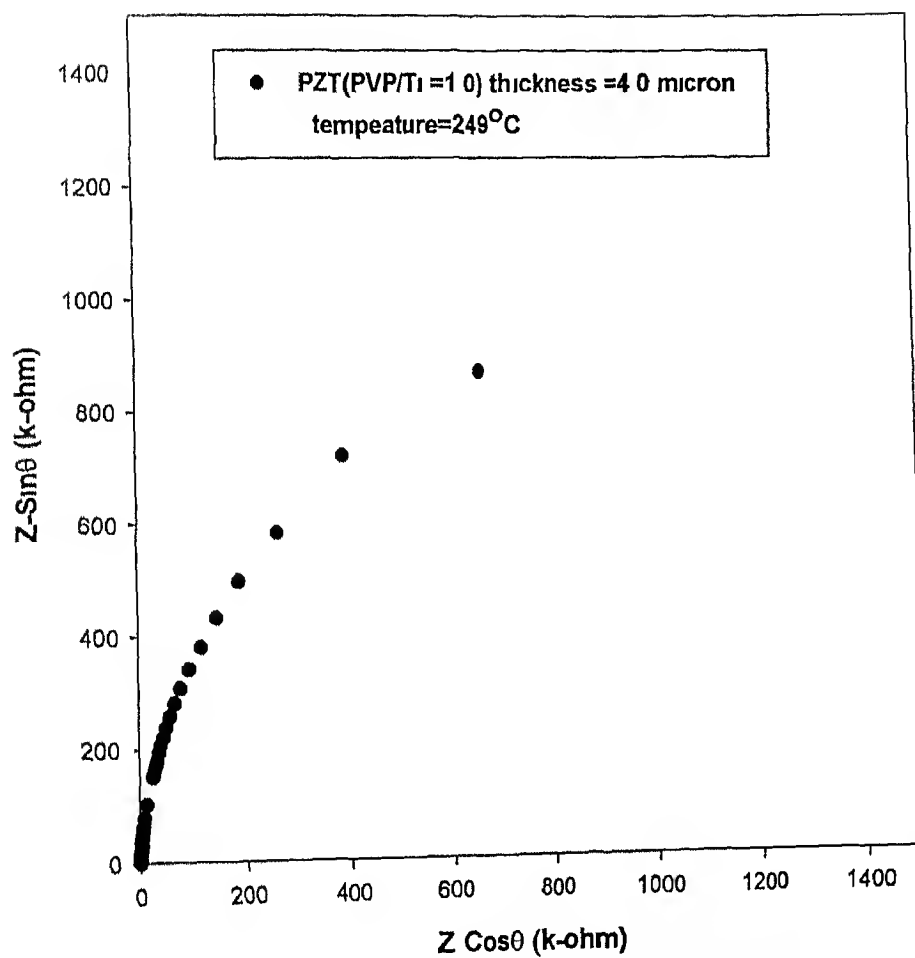


Fig 3 23 Cole Cole plot for PZT(PVP/Ti ≈ 1.0)  
(Sol Concentration ≈ 0.63M)

## Conclusion

- 1 The primary objective of this work was to prepare thick crack free film of PZT by the sol gel process. It has been found that by addition of the polymer polyvinyl pyrrolidone to the sol, film of thickness of  $0.5 \mu\text{m}$  can be obtained in single coating. Film up to  $11 \mu\text{m}$  thick have been obtained by 21 coatings. Without PVP, a film of  $10 \mu\text{m}$  thickness is obtained with difficulty using at least 25 coatings. Acetic acid is used during sol gel preparation of PZT films. It has been found in the present work that the amount of acetic acid drastically influence the dielectric properties of the films specifically a very high dielectric loss is obtained in these films. Also an anomaly in several properties is noted at a PVP/Ti concentration of 0.5. Several other conclusion from the study are as
- 2 Thicknesses of the films are found to increase with initial addition of PVP and become nearly constant, as the PVP concentration is further increased
- 3 The dielectric constant of the films increases rapidly on increasing the PVP (monomer)/Ti molar ratio from 0 to 0.5 and then becomes nearly constant
- 4 Large variation in dielectric constant is observed in the frequency range from 1 to 20 KHz. The dielectric constant is found to be nearly constant at frequency  $>30$  KHz but increases steeply as the frequency is decreased
- 5 Dielectric loss also decreases with increase in the frequency. Large variation in dielectric loss has been observed in 1.0 to 20 KHz frequency range

- 6 The films have significantly higher dielectric loss when the concentration of acetic acid is large
- 7 The dielectric constant of the films are found to increases with the film thickness from 150 for 4  $\mu\text{m}$  thick film to ~350 for 11.5  $\mu\text{m}$  thick film
- 8 The activation energy of grain conduction is 10 to 12 kJ/mole for most of the PZT samples except for the sample with PVP/TI ratio of 0.2 and 2.0 for which activation energies are 28.8 and 4.3 kJ/mole  
  
The activation energy for the grain boundary conduction tends to have values which vary between 3.0 to 25.0 kJ/mole  
  
However, these values are tentative and need to be confirmed
- 9 For films prepared using the higher concentration sol (0.63M) single incomplete arcs are obtained in the Cole Cole plots indicating that the relaxation processes are slow in the films

## **Future work**

In the present work the aim was used to prepare thick films by addition of PVP. The study should be extended further by investigating the microstructure, ferroelectric properties, C-V and I-V characteristics of the films. The drastic effect of acetic acid on the films properties is of special interest and should be further investigated.

## References

- 1 B M Melnic J D Cuchiaro, L D Mcmillan C A Paz De Araujo and J F Scott  
Process Optimization and Characterization of Device Worthy Sol Gel Based  
PZT for Ferroelectric Memories *Ferroelectrics* Vol 112 pp 329 351 1990
- 2 Yeur Luen Tu L M Calzada J Nicolas Phillips and J S Milne Synthesis and  
Electrical Characterization of Thin Films PT and PZT made from Diol Based Sol  
Gel Route ' *J Am Ceram Soc* Vol 79 no 2, pp 441 448 1996
- 3 Binmin Xu, L Eric Cross and D Ravichandran Synthesis of Lead Zirconate  
Titanate Stannate Antiferroelectric Thick Film by Sol Gel Process *J Am  
Ceram Soc* Vol 82, no 2, pp 306 312 1999
- 4 R Kurchania, and Steven J Milne Characterization of Sol Gel  $\text{Pb}(\text{Zr}_{0.53}\text{Ti}_{0.47})\text{O}_3$   
Films in the Thickness Range of 0.25 to 10  $\mu\text{m}$  ' *J Mater Res* Vol 14 no 5  
pp 1852 1858, 1999
- 5 Y L Tu, and S J Milne, 'Influence of Sol Synthesis Condition on the Electrical  
Properties of PZT Thin Films', *J Mater Sci Lett* Vol 14 no 12 pp 885 888  
1995
- 6 Del Monte, P Cheben, C P Grover and J D Mackenzie, Preparation and Optical  
Characterization of Thick Film Zirconia and Titania Ormosils *J Sol Gel Sci  
and Technology*, Vol 15 no 1, pp 73 85, 1999
- 7 J Koo, Sung Uk Kum, D S Yoon, K No and Byeong Soo Bae Effect of Heat  
Treatment on Formation of Sol Gel PZT Film for Optical Application *J Mater  
Res*, Vol 12, no 3, pp 812 818 1997

- 8 A Schonecker, H J Gesemann and L Seffner Low Sintering PZT Ceramic for Advanced Actuators , IEEE international Symposium on Application of Ferroelectrics 1996
- 9 K G Brooks M Kohli D V Taylor T Maeder, I Reaney A Kholkin P Muralt and N Setter, Sol Gel Deposition of PZT Thin Film on Ceramic  $ZrO_2$  Substrate', IEEE international Symposium on Application of Ferroelectrics Vol 2 pp 611 614 1996
- 10 T Futakuchi Y Matsui, and M Adachi, Preparation of  $0.92 PbZrO_3 - 0.03 PbTiO_3 - 0.05 Pb (Zn_{1/3}Nb_{2/3}) O_3$  Pyroelectric Thick Films by Screen Printing Jap J Appl Phys Vol 37, pp 5158 5161, 1998
- 11 S Sherrit, C R Savin, H D Wiederick and B K Mukherjee Plasma Sprayed Lead Zirconate Titanate Glass Composites', J Am Ceram Soc Vol 77 no 7 pp 1973 1975, 1994
- 12 T Kubota, K Tanaka, and Y Sakabe, Formation of  $Pb(ZrTi)O_3 - Pb(Zn Nb)O_3$  System Piezoelectric Thick Films in Low Temperature Firing Process Jap J Appl Phys Vol 38, pp 5535 5538, 1999
- 13 J Akedo, and M Lebedev, Microstructure and Electrical Properties of Lead Zirconate Titanate  $Pb(Zr_{0.52} Ti_{0.48})O_3$  Thick Films Deposited by Aerosol Deposition Method', Jap J Appl Phys, Vol 38, pp 5397 5401 1999
- 14 A Schroth, R Maeda, J Akedo, and M Ichiki, Application of Gas Jet Deposition Method to Piezoelectric Thick Film Miniature Actuator' Jap J Appl Phys Vol 37, pp 5342 5344, 1998



- 15 T Sweeney and R W Whatmore Electrophoretic Deposition of PZT Ceramic Films IEEE International Symposium on Application of Ferroelectrics Vol 1 pp 193 196 1996
- 16 Yumane Masayuki, 'Preparation of Thick PZT Ceramic Film by an Interfacial Polymerization , J Sol Gel Science and Technology, Vol 13 no (1 3) pp 821 825 1998
- 17 H Okino, T Nishikawa, M Shimizu T Horiuchi and K Matsushige Electrical Properties of Highly Stressed Epitaxial  $\text{Pb}(\text{ZrTi})\text{O}_3$  thin film on  $\text{MgO}(100)$  Jap J Appl Phys Vol 38 pp 5388 5391, 1999
- 18 K Amanuma, T Mori, and T Hase T Sakuma A Ochi and Y Miyasaka "Ferroelectric Properties of Sol Gel Derived  $\text{Pb}(\text{ZrTi})\text{O}_3$  Thin Films ' Jap J Appl Phys Vol 32, Part 1, no 9B pp 4150 4153 1993
- 19 Sung Gap Lee, In Gil Park, Seon Gi Bag and Yound Hie Lee Dielectric Properties of  $\text{Pb}(\text{ZrTi})\text{O}_3$  Heterolayered Films Prepared by Sol Gel Method Jap J Appl Phys, Vol 36, Part 1, no 11, pp 6880 6883 1997
- 20 T K Kundu and Joseph Ya Min Lee Thickness Dependent Electrical Properties of  $\text{Pb}(\text{Zr,Ti})\text{O}_3$  Thin Film Capacitors for Memory Device Application Journal of The Electrochemical Society, Vol 147, no 1 pp 326 329 2000
- 21 M I Maletto, L I Solovjeva, E P Turevskaya, and K A Vortilov Alkoxy Derived  $\text{Y}_2\text{O}_3$  Stabilised  $\text{ZrO}_2$  Thin Films ', Thin Solid Films, Vol 249, no 1, pp 1 5 1994
- 22 N Yu, P C McIntyre, C Paul, T E Levine P E Giannelis J W Mayer and M Nastasi, "Ion Beam Induced Epitaxial Crystallization of Sol Gel Zirconia Thin

- Films on Yttria Stabilized Zirconia Philosophical Magazine Letters Vol 73  
no 6 pp 359 368 1996
- 23 A Mehner, H Kluemper Westkamp, F Hoffmann, and P Mayr Crystallization  
and Residual Stress Formation in Sol Gel Derived Zirconia Films Thin Solid  
Films, Vol 308 309 pp 369 368 1997
  - 24 Y Shichi, S Tanimoto, T Goto, K Kuroiwa, and Y Tarui Interaction of  $\text{PbTiO}_3$   
films with  $\text{Si}$  Substrate, Jap J Appl Phys Vol 33 pp 5172 5177 1994
  - 25 H Kozuka, and M Kajimura Single Step Dip Coating of Crack Free  $\text{BaTiO}_3$   
films  $>1 \mu\text{m}$  Thick Effect of Poly (vinylpyrrolodone) on Critical Thickness J  
Am Ceram Soc, Vol 83 [5], pp 1056 1062 2000
  - 26 Zhan Jie -Wang, R Maeda, and K Kikuchi Preparation and characterization of  
Sol Gel Derived PZT Thin Film for Micro Actuators Proceeding of SPIC The  
International Society for Optical Engineering Vol 3680, no 2, pp 948 955 1999
  - 27 Sung Gap Lee, K T Shim, and Y H Lee Preparation and Characterization of  
Lead Zirconate Titanate Heterolayered Thin Films on  $\text{Pt/Ti/SiO}_2/\text{Si}$  Substrate by  
Sol Gel Method', Jap J Appl Phys Part1 Regular Papers and Short Notes and  
Review Papers, Vol 39 no 1(A), pp 217 218 1999
  - 28 M I Reaney, D V Taylor, and K G Brooks, Ferroelectric PZT thin Films by Sol  
Gel Deposition', J Sol Gel Science and Technology, Vol 13 no 1 30 pp 813  
820, 1998
  - 29 J F Fernandez, E Nieto, C Moure, and P Duran Processing of Porous Dense PZT  
Thick Films on  $\text{Al}_2\text{O}_3$  Substrate', IEEE International Symposium on Application  
of Ferroelectrics, pp 49 52, 1994

- 30 J F Fernaandez, E Nieto C Moure P Durane and R E Newnham Processing and Microstructure of Porous and Dense PZT Thick Films on  $\text{Al}_2\text{O}_3$  J Materials Science Vol 30 no 21 pp 5399 5404 1995
- 31 J B Jaffe W R Cook and H Jaffe *Piezoelectric Ceramic* 1971 Academic Press
- 32 Yeu Luen Tu M L Calzada, N J Phillips and S J Milne Synthesis and Electrical Characterization of Thin Film of PT and PZT Made From Diol Based Sol Gel Route", J Am Ceram Soc Vol 79 (12) pp 141 148 1996
- 33 Jie Luo, D P Almond, and R Stevens Ionic Mobilities and Association Energies from an Analysis of Electrical Impedance of  $\text{ZrO}_2$   $\text{Y}_2\text{O}_3$  alloys J Am Ceram Soc, Vol 83 (7) pp 1703 1708, 2000
- 34 J R MacDonald *Impedance Spectroscopy Emphasizing Solid Materials and System*", Willy, New York, 1987

# Appendix

## **Appendix (1) Silicon wafer cleaning**

RCA cleaning is used to clean silicon wafer. This process consists of the following steps

### **(A) Standard cleaning (1)**

A mixture of distilled water, unstabilised  $\text{H}_2\text{O}_2$  (30%) and  $\text{NH}_4\text{OH}$  (27%) in ratio of 5:1:1 is used. This solution etches the thermally grown oxide at the rate of 0.1 nm/min. Also it removes all the organic contamination. Si wafer is submerged in this standard cleaning (1) solution at temperature  $75^\circ\text{C} - 80^\circ\text{C}$  for 30 min. After cleaning, Si wafer is transferred to another solution of HF and distilled water mixture in ratio of 50:1.

### **(B) (HF – $\text{H}_2\text{O}$ ) mixture**

During cleaning by standard solution (1), some native oxide ( $\text{SiO}_2$ ) is formed. To remove this native oxide, HF –  $\text{H}_2\text{O}$  (50:1) mixture is used. Silicon wafer is dipped in HF solution then rinsed in distilled water for 15 min. Here silicon dioxide ( $\text{SiO}_2$ ) is removed and silicon surface is exposed. After cleaning, Si wafer is transferred to standard cleaning solution (2).

### **(C) Standard cleaning solution (2)**

It is a mixture of  $\text{H}_2\text{O}$ ,  $\text{H}_2\text{O}_2$  and  $\text{HCl}$  in ratio of 6:1:1. This mixture is used to remove the heavy metal and ionic contamination. The processing temperature should be around  $75^\circ\text{C}$  to  $80^\circ\text{C}$ . After cleaning the Si (100) substrate, it is dried in open air and kept in small plastic container. This cleaned substrate is used as substrate for film deposition.

In present work the above process was not used. Instead of the Si(100) wafer was cut by diamond tool and cleaned with a mixture of HF and distilled water (50:1). For 20 minutes rinsed in distilled water and dried.

## **Appendix (2) Calculation of the amount of ingredients used for the preparation of sol for ZrO<sub>2</sub> coating**

### **(1) Zr(n)-propoxide**

We have to prepare a solution of 0.5 M and total solution volume should be 20 ml

1000 ml solution requires = 0.5 mole

$$20 \text{ ml solution requires} = \frac{0.5}{1000} * 20 \text{ mole}$$

$$= 0.01 \text{ Mole}$$

$$0.01 = \frac{\text{Weight of Zr(n-propoxide)}}{327.57}$$

$$\text{Wt of Zr(n-propoxide)} = \text{Volume} * \text{Density}$$

$$\text{Volume of Zr(n-Propoxide)} = \frac{3.2757}{1.05}$$

$$= 3.119 \text{ ml}$$

### **(B) DEA (Diethanol amine)**

Molar concentration ratio of DEA and Zr(n-propoxide) should be 0.74

$$\text{So concentration of DEA} = 0.74 * 0.5 \text{ M}$$

$$=0.37 \text{ M}$$

1000 ml of solution requires =0.37 mole of DEA

$$20 \text{ ml of solution requires DEA} = \frac{0.37}{1000} * 20 \text{ mole}$$

$$=0.0074 \text{ mole}$$

$$\frac{\text{Weight of DEA}}{\text{Molecular weight of DEA}} = 0.0074$$

$$\text{Wt of DEA} = 0.0074 * 105.14$$

$$=0.7780 \text{ gm}$$

$$\text{Volume of DEA} = \frac{\text{Weight of DEA}}{\text{Density of DEA}}$$

$$= \frac{0.7780}{1.098} \text{ ml}$$

$$=0.7085 \text{ ml}$$

### (C) For water

$$\text{Water concentration} = 0.9 \text{ M}$$

1000 ml solution contain =0.9 mole of H<sub>2</sub>O

$$20 \text{ mole of solution contain} = \frac{0.9}{1000} * 20 \text{ mole}$$

$$=0.018 \text{ mole of H}_2\text{O}$$

$$\text{Weight of water} = \text{Mole of H}_2\text{O} * \text{molecular wt of water}$$

$$=0.018 * 18$$

$$=0.324 \text{ gm}$$

$$\text{Volume of water} = \frac{\text{Weight of water}}{\text{Density of water}}$$

$$= \frac{0.324}{1.00} \text{ ml}$$

$$= 0.324 \text{ ml}$$

**(D) For isopropyl alcohol**

Total volume of the sol is made up to by adding isopropyl alcohol

Volume of isopropyl alcohol = 20 - [ Volume of Zr(n Propoxide + DEA+ water ]

$$= 20 - [3.119 + 0.708 + 0.324] \text{ ml} \Rightarrow 15.87$$

**Appendix (3)· Calculation of the amount of ingredients used for the preparation of sol for  $\text{Pb}_{1.05}(\text{Zr}_{0.535}\text{Ti}_{0.465})\text{O}_3$  (PZT)coating**

$\text{Pb}_{1.05}(\text{Zr}_{0.535}\text{Ti}_{0.465})\text{O}_3$  0.01M sol preparation

**(1) PVP (poly vinylpyrrolidon)**

In present work, different ratios of PVP/Ti were used. Thus for a 1:1 ratio the amount of PVP for the composition  $\text{Pb}_{1.05}(\text{Zr}_{0.535}\text{Ti}_{0.465})\text{O}_3$  to prepare a sol of concentration 0.01M is 0.516 gm

Molecular wt of poly vinylpyrrolidon monomer is =111 gm

Since mole ratio of PVP and Ti(n propoxide)is 1:1

Mole of Ti in for  $\text{Pb}_{1.05}(\text{Zr}_{0.535}\text{Ti}_{0.465})\text{O}_3$  0.01M sol =mole of PVP

$$0.01 \times 0.465 = \frac{\text{Weight of PVP}}{\text{Mol. wt of PVP}}$$

$$\text{Amount of PVP} = 0.01 \times 0.465 \times 111$$

$$= 0.516 \text{ gm of PVP}_{(\text{monomer})}$$

**(2)  $\text{Pb}(\text{CH}_3\text{COO})_2 \cdot 3\text{H}_2\text{O}$**

Mole of Pb in  $\text{Pb}_{1.05}(\text{Zr}_{0.535}\text{Ti}_{0.465})\text{O}_3$  0.01M sol = Mole of  $\text{Pb}(\text{CH}_3\text{COO})_2 \cdot 3\text{H}_2\text{O}$

$$0.01 \times 1.05 = \frac{\text{Amount of } \text{Pb}(\text{CH}_3\text{COOH})_2 \cdot 3\text{H}_2\text{O}}{\text{Mol Wt of } \text{Pb}(\text{CH}_3\text{COOH})_2 \cdot 3\text{H}_2\text{O}}$$

$$\text{Amount of } \text{Pb}(\text{CH}_3\text{COO})_2 \cdot 3\text{H}_2\text{O} = 0.01 \times 1.05 \times 379.33$$

$$= 3.98 \text{ gm}$$

$$\text{As the yield of } \text{Pb}(\text{CH}_3\text{COO})_2 \cdot 3\text{H}_2\text{O} \text{ is } 99.97\%, \text{ the actual amount} = \frac{100}{99.97} \times 3.98$$

**(3)  $\text{Zr}(\text{n propoxide})$**

Mole of Zr in  $\text{Pb}_{1.05}(\text{Zr}_{0.535}\text{Ti}_{0.465})\text{O}_3$  0.01M sol = mole of  $\text{Zr}(\text{n Propoxide})$

$$0.01 \times 0.535 = \frac{\text{Wt of } \text{Zr}(\text{n-Propoxide})}{\text{Mol Wt of } \text{Zr}(\text{n-Propoxide})}$$

$$\text{Amount of } \text{Zr}(\text{n propoxide}) = 0.01 \times 0.535 \times 327.58$$

$$= 1.753 \text{ gm}$$

As the yield of  $\text{Zr}(\text{n propoxide})$  is 74.88

$$\text{So actual amount of } \text{Zr}(\text{n propoxide}) = \frac{100}{74.88} \times 1.752 \text{ gm}$$

$$= 2.34 \text{ gm}$$

**(4)  $\text{Ti}(\text{4 butoxide})$**

Mole of Ti in  $\text{Pb}_{1.05}(\text{Zr}_{0.535}\text{Ti}_{0.465})\text{O}_3$  0.01M sol = Mole of  $\text{Ti}(\text{n butoxide})$

$$0.01 \times 0.465 = \frac{\text{Wt of } \text{Ti}(\text{4-butoxide})}{\text{Mol Wt of } \text{Ti}(\text{4-butoxide})}$$

$$\text{Amount of } \text{Ti}(\text{4 butoxide}) = 0.01 \times 0.465 \times 340 \text{ gm}$$



$$=1.58 \text{ gm}$$

As yield of Ti(4 butoxide) = 99.98%

$$\text{So actual amount of Ti(4 butoxide)} = \frac{100}{99.98} * 1.58$$

$$=1.582 \text{ gm}$$

#### (5) For $\text{CH}_3\text{COOH}$

The ratio  $\text{Pb}(\text{CH}_3\text{COOH})_2 \cdot 3\text{H}_2\text{O}$  and  $\text{CH}_3\text{COOH}$  equal to 1:4 used in present work

$$\frac{\text{MolWt. of } \text{Pb}(\text{CH}_3\text{COOH})_2 \cdot 3\text{H}_2\text{O}}{\text{MolWt. of } \text{CH}_3\text{COOH}} = \frac{1}{4}$$

$$\frac{\frac{\text{Amount of } \text{Pb}(\text{CH}_3\text{COOH})_2 \cdot 3\text{H}_2\text{O}}{\text{MolWt. of } \text{Pb}(\text{CH}_3\text{COOH})_2 \cdot 3\text{H}_2\text{O}}}{\frac{\text{Amount of } \text{CH}_3\text{COOH}}{\text{MolWt. of } \text{CH}_3\text{COOH}}} = \frac{1}{4}$$

$$\frac{\frac{3.99}{379.33}}{\frac{\text{Amount of } \text{CH}_3\text{COOH}}{60.05}} = \frac{1}{4}$$

$$\text{Amount of } \text{CH}_3\text{COOH} = 2.52 \text{ gm}$$

In addition to this, 1.2 gm acetic acid was also added to the mixture of alkoxide during sol preparation as depicted in the flow sheet. Additional amount of acetic acid was used for dilution of the prepared sol as described in the text.

133647

133647  
Date Slip

The book is to be returned on  
the date last stamped

